



ELSEVIER

Precambrian Research 90 (1998) 159–185

**Precambrian
Research**

Hornblende $^{40}\text{Ar}/^{39}\text{Ar}$ geochronology across terrane boundaries in the Sveconorwegian Province of S. Norway

Bernard Bingen ^{a,*}, Ariel Boven ^b, Lea Punzalan ^b, Jan R. Wijbrans ^c, Daniel Demaiffe ^a

^a *Département des Sciences de la Terre et de l'Environnement, CP 160/02, Université Libre de Bruxelles, 1050 Brussels, Belgium*

^b *Afdeling Geochronologie, Vrije Universiteit Brussel, 1050 Brussels, Belgium*

^c *Department of Petrology and Isotope Geology, Faculty of Earth Sciences, Vrije Universiteit, 1081 HV Amsterdam, The Netherlands*

Received 4 March 1997; accepted 12 February 1998

Abstract

Hornblende incremental heating $^{40}\text{Ar}/^{39}\text{Ar}$ data were obtained from augen gneiss and amphibolite of the Sveconorwegian Province of S. Norway. In the Rogaland–Vest Agder and Telemark terranes, four pyroxene-rich samples, located close (≤ 10 km) to the anorthosite–charnockite Rogaland Igneous Complex, define an age group at $916 \pm 12/-14$ Ma and six samples distributed in the two terranes yield another group at $871 \pm 8/-10$ Ma. The first age group is close to the reported zircon U–Pb intrusion age of the igneous complex (931 ± 2 Ma) and the regional titanite U–Pb age (918 ± 2 Ma), whereas the second group overlaps reported regional mineral Rb–Sr ages (895–853 Ma) as well as biotite K–Ar ages (878–853 Ma). In the first group, the comparatively dry parageneses of low-*P* thermal metamorphism (M2) associated with the intrusion of the igneous complex are well developed, and hornblende $^{40}\text{Ar}/^{39}\text{Ar}$ ages probably record a drop in temperature shortly after this phase. In other hornblende + biotite-rich samples, with presumably a higher fluid content, the hornblende ages are probably a response to hornblende–fluid interaction during a late Sveconorwegian metamorphic or hydrothermal event. A ca 220 m.y. diachronism in hornblende $^{40}\text{Ar}/^{39}\text{Ar}$ ages is documented between S. Telemark (ca 870 Ma) and Bamble (ca 1090 Ma). Differential uplift between these terranes was mostly accommodated by shearing along the Kristiansand–Porsgrunn shear zone. The final stage of extension along this zone occurred after intrusion of the Herefoss post-kinematic granite at 926 ± 8 Ma. On the contrary, the southern part of the Rogaland–Vest Agder and Telemark terranes share a common cooling evolution as mineral ages are similar on both sides of the Mandal–Ustaoset Line the tectonic zone between them. The succession within 20 m.y. of a voluminous pulse of post-tectonic magmatism at 0.93 Ga, a phase of high-*T*–low-*P* metamorphism at 0.93–0.92 Ga, and fast cooling at a regional scale ca 0.92 Ga, suggests that the southern parts of Rogaland–Vest Agder and Telemark were affected by an event of post-thickening extension collapse at that time. This event is not recorded in Bamble. © 1998 Elsevier Science B.V.

Keywords: Anorthosite; Ar/Ar; Grenvillian orogeny; Shear zones; Southern Norway; Terranes

* Corresponding author. Present address: Norges Geologiske Undersøkelse, Leiv Eirikssons vei 39, 7040 Trondheim, Norway.
Fax: +47 73 921620; e-mail: bernard.bingen@ngu.no

1. Introduction

The Sveconorwegian Province of the Baltic Shield is made up of an assemblage of deeply eroded, Mesoproterozoic terranes reworked and displaced during the Sveconorwegian orogeny, that is, during the 1.25–0.90 Ga period. The terranes are predominantly made up of high-grade gneiss complexes. Recent geochronological and structural data have shown that Sveconorwegian medium- to high-grade metamorphism was penetrative over large areas of the province but that it developed diachronously in different terranes (Bingen et al., 1990; Kullerud and Dahlgren, 1993; Page et al., 1996; Romer, 1996).

In the west of the province, in S. Norway, the Rogaland–Vest Agder, Telemark and Bamble terranes are separated by two major tectonic zones with contrasting styles (Fig. 1): the Mandal–Ustaoset Line (Mandal Line), between Rogaland–Vest Agder and Telemark (Sigmond, 1985) and the Kristiansand–Porsgrunn shear zone, between Telemark and Bamble (e.g. Starmer, 1991). The latter is a mylonitic thrust zone, subsequently cut by a zone of normal faults. The Mandal Line is an orogen-parallel polyphase tectonic zone, well defined by highly sheared gneisses and fault zones for most of its northern part. To the south, it is marked by a broad, deep-seated amphibolite-facies banded gneiss unit in line with the northern shear zone.

Two granulite-facies domains with a progressive amphibolite- to granulite-facies transition zone are described in these terranes (Fig. 1). In the coastal region of Bamble, regional medium-*P* granulite-facies metamorphism occurred at 1.15–1.10 Ga (Kullerud and Dahlgren, 1993; Nijland and Maijer, 1993). In SW Rogaland–Vest Agder, high-*T*–low-*P* granulite-facies metamorphism is significantly younger (Pasteels et al., 1979; Demaiffe and Michot, 1985; Verschure, 1985). Its origin and detailed geochronology are controversial as interference exists between contact metamorphism related to the intrusion of the anorthosite–charnockite Rogaland Igneous Complex and Sveconorwegian regional metamorphism (Tobi et al., 1985; Maijer, 1987).

Hornblende stepwise heating $^{40}\text{Ar}/^{39}\text{Ar}$ geochronology has been conducted on gneisses from the Rogaland–Vest Agder, Telemark and Bamble terranes and complements a U–Pb geochronological study in the region. The objective is to better constrain the tectonothermal evolution of these terranes and to better understand the significance of major tectonic zones during orogenesis and uplift. Special emphasis is placed on the gneisses surrounding the Rogaland Igneous Complex as the cooling path following intrusion gives information on the tectonic setting of massif-type anorthosites.

2. Geological setting

The Rogaland–Vest Agder, Telemark and Bamble terranes (Fig. 1) consist predominantly of amphibolite- to granulite-facies gneiss complexes. A low-grade supracrustal complex—the Telemark Supergroup—is exposed in the northern part of Rogaland–Vest Agder and Telemark (Demaiffe and Michot, 1985; Falkum, 1985; Verschure, 1985). The gneiss complexes are made up of elongated units of augen, banded, migmatitic and granitic gneisses, intercalated with minor amphibolite, quartzite and marble units. The oldest units were probably affected by high-grade metamorphism during the Kongsbergian event [1.75–1.35 Ga; Starmer (1991)].

The magmatic activity linked to the Sveconorwegian orogeny mainly comprises small gabbro intrusions (de Haas et al., 1993) as well as leucogranite and K-feldspar megacrystic granitoid plutons which were variously gneissified. At least three suites of megacrystic granitoid deformed to augen gneiss are present (Pedersen, 1981; Kullerud and Dahlgren, 1993; Heaman and Smalley, 1994; Zhou et al., 1995; Bingen and van Breemen, 1998):

- (1) the first suite, characterized by an A-type geochemical affinity, intruded between 1187 ± 2 Ma (Gjerstad augen gneiss) and 1152 ± 2 Ma (Gjeving charnockite; zircon U–Pb ages) in Telemark, Bamble and Rogaland Vest Agder;
- (2) the second, a voluminous suite, represented by the Feda augen gneiss, has a high-K calc-

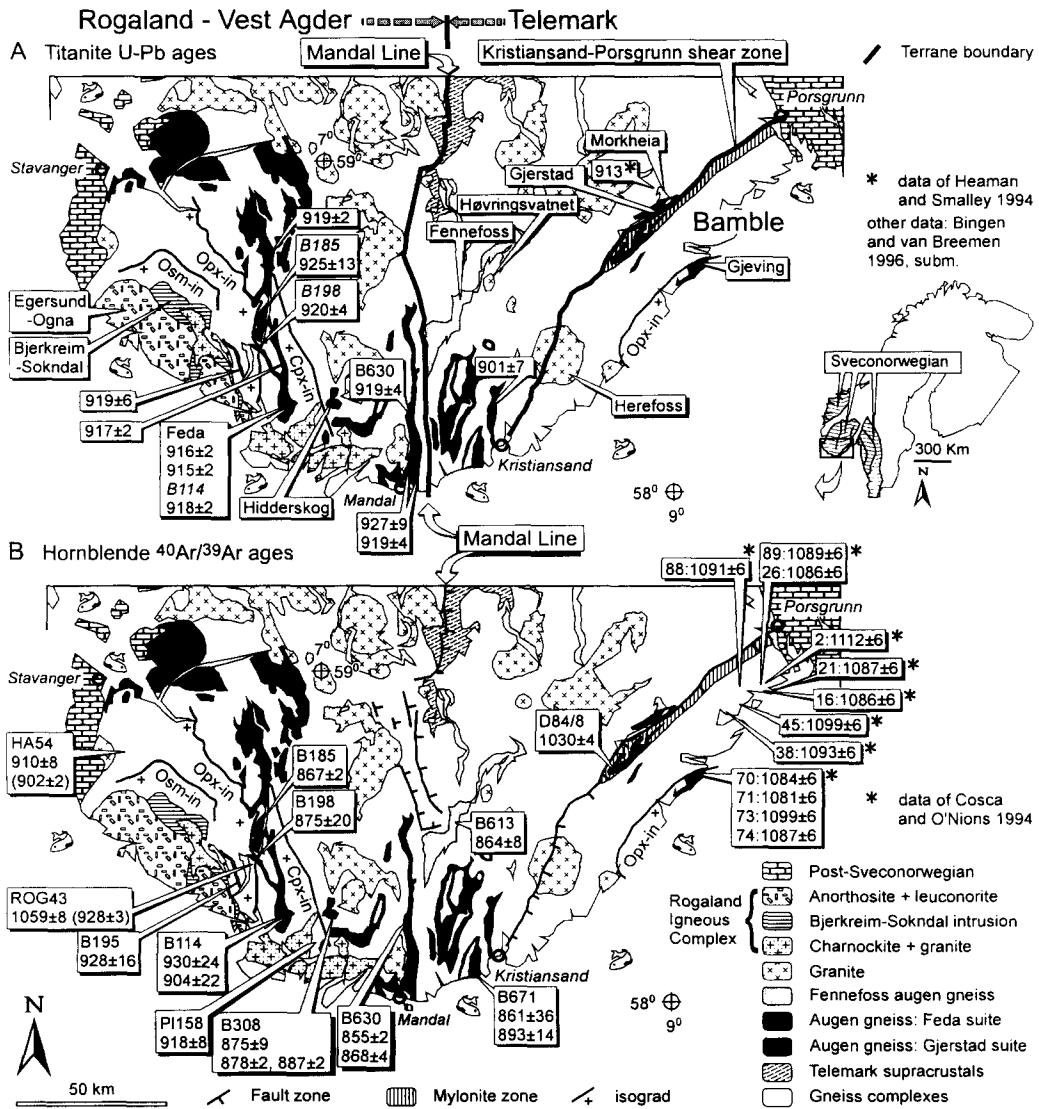


Fig. 1. (A) Geological sketchmap of the Sveconorwegian Province of S. Norway with terrane boundaries and published titanite U–Pb ages (the most concordant fraction for each sample is selected). Osm-in stands for osumilite-in isograd. (B) Sketchmap with tectonic zones, sample locations and hornblende $^{40}\text{Ar}/^{39}\text{Ar}$ plateau or single-step ages (intercept age of inverse isochron between brackets for ROG43 and HA54).

alkaline affinity; it crystallized at $1050 \pm 2/-8$ Ma in Rogaland–Vest Agder (zircon U–Pb age); it points to a subduction setting at 1.05 Ga;

(3) the Fennefoss augen gneiss of Telemark represents the third suite; it crystallized at $1035 \pm 2/-3$ Ma (zircon U–Pb age) and is

geochemically intermediate between calc-alkaline and alkaline.

Both the gneiss complexes and the Telemark Supergroup are cut by a large number of post-tectonic intrusions. A pegmatite intruded in Bamble at $1060 \pm 8/-6$ Ma [euxinite U–Pb age;

Baadsgaard et al. (1984)]; the first post-tectonic granite plutons crystallized at 1.00 Ga in Telemark and Bamble [Grimstad granite at 997 ± 12 Ma; zircon U–Pb age; Kullerud and Dahlgren (1993)] and 0.98 Ga in Rogaland–Vest Agder [Holum granite at 980 ± 33 Ma; Rb–Sr isochron; Wilson et al. cited in Verschure (1985)]. Large volumes of magma were emplaced at 0.93 Ga: the Herefoss granite in Bamble [926 ± 8 Ma; titanite Pb–Pb age; Andersen (1997)], the Høvringsvatn complex in Telemark [945 ± 53 and 900 ± 53 Ma; Rb–Sr isochron; Pedersen (1981)] and the Rogaland Igneous Complex [references and review in Duchesne et al. (1985)]. The intrusion of anorthosite bodies at 931 ± 2 Ma [zircon and baddeleyite U–Pb ages; Schärer et al. (1996)] is coeval with crystallization of associated charnockite plutons [zircon U–Pb ages; Pasteels et al. (1979)], indicating that the whole complex was emplaced during a short magmatic event. It was closely followed by pegmatite intrusion at 914 ± 6 Ma [Rymteland pegmatite; uraninite U–Pb age; Pasteels et al. (1979)].

3. Metamorphism

In Rogaland–Vest Agder, metamorphic grade increases westwards (Tobi et al., 1985). This progression is marked by a succession of isograds [Fig. 1; Tobi et al. (1985); Bingen et al. (1990)]: from east to west, clinopyroxene-in (Cpx-in) in augen gneiss, orthopyroxene-in (Opx-in) in leucocratic gneiss and augen gneiss, osumilite-in in metapelitic gneiss close to the Rogaland Igneous Complex. According to Tobi et al. (1985) and Maijer (1987), this pattern is the result of three metamorphic phases: M1, M2, M3. M1 reached upper-amphibolite- to granulite(?) facies and is reflected by the oldest recognizable mineral assemblages, for example hornblende + biotite \pm Cpx \pm Opx(?) in intermediate to mafic rocks or biotite \pm garnet \pm sillimanite in metapelites. M2 is characterized by high-*T*-low-*P* granulite-facies associations, for example, osumilite + spinel + Opx, and spinel + quartz in some paragneiss units. M3 is a late phase associated with various coronitic textures developed in metapelitic rocks, for example, breakdown of osumilite into symplectite of

cordierite + K-feldspar + Opx or thin garnet rims around green spinel. The lack of major deformation associated with osumilite-bearing associations and the parallelism between the osumilite-in isograd and the external contact of the Rogaland Igneous Complex support the hypothesis that M2 corresponds to a phase of thermal metamorphism related to the intrusion of this complex. Whether M1 reached granulite-facies conditions or not, is unclear in the model of Tobi et al. (1985): Opx-bearing associations in paragneiss and mafic gneiss are possibly attributed to M1. The Opx-in isograd diverges northwards from the osumilite-in isograd or from the contact of the igneous complex, indicating that it can be related to the older M1 event and unrelated to intrusion of the complex. To the west of the osumilite-in isograd, *P*-*T* estimates using mineral equilibria are close to 5.5 kbar–800–850°C for M2 and 3 kbar–550–700°C for M3 assemblages (Jansen et al., 1985; Holland et al., 1996).

Zircon U–Pb data in garnet-bearing migmatitic gneisses to the west of the osumilite-in isograd point to anatexis at ca 1.03 Ga (Wielens et al., 1981). The oldest monazite generation in orthogneiss to the west of the Opx-in and osumilite-in isograds, crystallized at 1024–997 Ma (Bingen and van Breemen, in press). If the short duration of anorthosite magmatism at 931 ± 2 Ma is accepted (Schärer et al., 1996), the range of ages obtained for zircon and monazite does not reflect a phase of contact metamorphism but should rather be related to the main Sveconorwegian orogenic phase, bracketed between the emplacement of orogenic granitoids at 1.05 Ga and the first post-kinematic granite at 0.98 Ga. Bingen and van Breemen (in press) defend the hypothesis that regional metamorphism (probably M1) largely reached granulite-facies conditions at 1.025–1.00 Ga. So far, the ages of specific mineral associations attributed to M2 and M3 are not well constrained: an osumilite K–Ar age of 987 ± 30 Ma is inconclusive (Maijer, 1987). Nevertheless, monazite crystallization at 930–925 Ma is probably linked to the M2 phase (Bingen and van Breemen, in press).

In Bamble, metamorphic grade increases south-eastwards. Four main isograds were mapped [sum-

mary in Nijland and Maijer (1993)] and four Sveconorwegian metamorphic phases (M1–M4) recognized in the core of the domain (Knudsen, 1996). Peak metamorphic conditions (M2) reached 7.1 ± 0.4 kbar– $750 \pm 30^\circ\text{C}$ in amphibolite-facies and 7.4 ± 1.6 kbar– $840 \pm 50^\circ\text{C}$ in the core of the granulite-facies domain (Nijland and Maijer, 1993; Knudsen, 1996). This granulite-facies event is bracketed by the intrusion of the Gjeving charnockite at 1152 ± 2 Ma, metamorphic zircon overgrowths at 1105 ± 8 Ma and a garnet–whole-rock–feldspar Sm–Nd internal isochron at 1098 ± 7 Ma (Kullerud and Dahlgren, 1993).

In the south of Telemark, *P–T* conditions and timing of amphibolite-facies metamorphism in the gneiss complex are poorly constrained. The Telemark Supergroup is affected by low-grade metamorphism.

4. Sampling and petrography

Coarse-grained samples with millimetre-sized hornblende crystals were chosen from the gneiss complexes of S. Norway (Fig. 1, Appendix A). At the southwestern end of Rogaland–Vest Agder, three samples from amphibolite layers and lenses in banded gneiss sequences were collected. Banded gneiss units are presumably Kongsbergian in age. To the west of the Opx-in isograd, there is evidence for at least two generations of pyroxene in metabasic rocks (Vander Auwera, 1993). Quartz-free mafic layers in folded banded gneiss sequences are commonly bordered at the contact of quartz-bearing layers, by a pyroxene-rich and amphibole-poor rim. The rim has constant thickness (5–10 mm) and thus post-dates any deformation. The formation of the rim is associated with dehydration and is controlled by SiO_2 diffusion between layers. It can be attributed to M2 thermal metamorphism. The core of the quartz-free layers displays a hornblende + biotite association with minor amount of Opx and Cpx; this granulite facies assemblage can be tentatively attributed to M1.

Nine samples of the three suites of augen gneiss were selected. These rocks were targeted as they intruded and were gneissified during Sveconorwegian times and, thus, underwent a compara-

tively short tectonothermal evolution. Augen gneiss bodies are almost concordant with regional structures. In the core of most bodies, poorly deformed zones where the igneous texture of K-feldspar phenocryst-bearing granodiorite is preserved, occur locally. Elsewhere, the regional gneissic foliation is variably marked; along the Kristiansand–Porsgrunn shear zone, mylonitic fabrics are reported. All samples were collected from homogeneous outcrops, preferentially in the less deformed zones of the bodies.

Augen gneiss bodies display a biotite ± hornblende magmatic association. Hornblende is commonly observed as inclusions in K-feldspar phenocrysts indicating its magmatic origin. In the 1.19–1.15 Ga Gjerstad suite, Opx of magmatic origin is commonly observed. In the 1.05 Ga Feda suite in Rogaland–Vest Agder, the colour of hornblende changes from green in amphibolite-facies to brown in granulite-facies. Amphibole has edenitic- to pargasitic-hornblende compositions with 6.5 ± 0.1 Si atoms in the structural formula and an average Ca/K ratio of 6.70 ± 0.92 [average of 14 samples; formula calculated on the basis of 23 O; Fig. 2; Bingen (1988)]. The Mg/(Mg + Fe^{2+}) ratio increases from 0.60 ± 0.07 to the east of the Cpx-in isograd to 0.69 ± 0.04 to the west of this isograd and to 0.77 ± 0.07 to the west of the Opx-in isograd (Fig. 2). There is no significant compositional difference between hornblende inclusions in K-feldspar megacrysts and matrix hornblende. These two features suggest that hornblende composition is homogeneous at the sample scale and characteristic of equilibrium metamorphic conditions (Bingen et al., 1990). In the Feda suite, pyroxenes are of metamorphic origin. The two pyroxenes granulite-facies association probably formed during M1, as in other granodioritic-granitic gneiss units. Cpx commonly displays hornblende inclusions, or surrounds hornblende aggregates to the west of the Cpx-in isograd (Bingen et al., 1990). The local preservation of these rims is compatible with Cpx growth during M2 thermal metamorphism. On the other hand, the pyroxene/hornblende ratio is extremely variable in the Feda suite to the west of the Cpx-in isograd [$0.12 < \text{Px}/(\text{Px} + \text{Hbl}) < 0.87$; Bingen et al. (1996)]; it is independent of the rock composition, indicat-

Hornblende in 1.05 Ga Feda suite

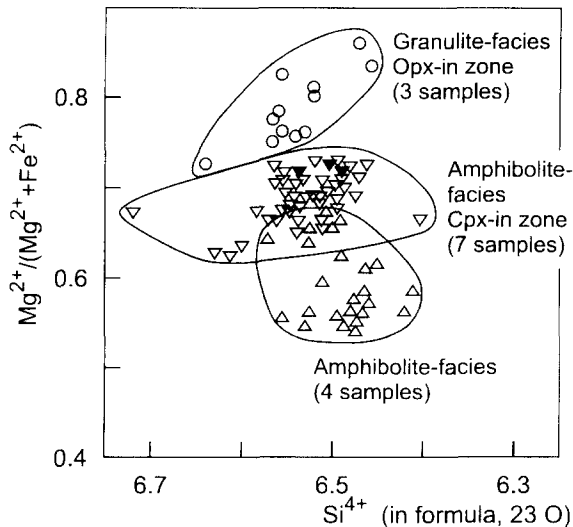


Fig. 2. Microprobe analyses of hornblende from 15 augen gneiss samples of the Feda suite showing the increase of $Mg^{2+}/(Mg^{2+} + Fe^{2+})$ ratio with increasing metamorphic grade [data of Bingen (1988)]. The composition of hornblende inclusions in K-feldspar megacrysts [sample 1a of Bingen (1988); close to sample B114 of this study; \blacktriangledown] is similar to matrix hornblende for this sample and other samples of the Cpx-in zone. Each symbol represents one analysis.

ing that breakdown of amphibole (during M2?) was dependent on local environmental conditions.

5. Methods

5.1. Analytical method

Final separates of clear, inclusion free, hornblende were obtained by hand-picking and were rinsed in acetone and deionized water. $^{40}Ar/^{39}Ar$ step-heating analyses of all but three samples were performed at the Vrije Universiteit Brussel. Two splits of most separates, together with aliquots of MMhb-1 hornblende standard, CaF_2 and K_2SO_4 salt monitors, were wrapped in Al-foil, loaded in a vacuum sealed quartz vial and irradiated under Cd-shielding within channel G240 of the BR2 reactor of the Belgian Nuclear Research Centre in Mol, for 3.49 days. The neutron flux was monitored using unpurified splits of MMhb-1. Among

the many standard ages reported for this sample (Baksi et al., 1996), the conventional K–Ar age of 513.9 ± 2.3 Ma has been used [Lanphere (personal communication) cited in Baksi et al. (1996)].

Gas was extracted using a resistance furnace. The samples were incrementally step-heated in a tantalum crucible. Temperature-steps were determined with a 5% W/Re–26% W/Re thermocouple. Released gases were purified by exposure to a Ti-getter within a temperature gradient as well as to heated and cold Zr–Al getters. They were measured with a MAP 216 mass spectrometer operated in static mode and equipped with a Baur-Signer source, a Johnston electron multiplier and a retractable Faraday cup. The abundance of the ^{40}Ar to ^{36}Ar isotopes was determined through linear extrapolation at zero time of peak intensities during 15 sequential scans. Details on the analytical procedures are presented in Boven et al. (submitted).

Three samples (HA54, PI158 and ROG43) were irradiated at the HIFAR reactor of the Australian Atomic Energy Commission (Lucas Heights NSW, Australia) during two full cycles of HIFAR. They were analysed at the Australian National University argon geochronology laboratory following the procedure described in Wijbrans and McDougall (1987). In this case the standard biotite GA1550 with a K–Ar age of 97.9 ± 0.7 Ma, corresponding to the recommended value of Baksi et al. (1996), was used as a neutron flux monitor.

The data were corrected for mass discrimination, interfering Ca, K, and Cl derived Ar isotopes, and decay of ^{37}Ar and ^{39}Ar from the time of irradiation (Tables 1–12). The ages were calculated using decay constants recommended by Steiger and Jäger (1977). The plateau ages quoted are weighted mean values for at least three consecutive steps, representing at least 60% of released ^{39}Ar . Uncertainties are quoted at the 2σ level and account for the analytical errors including the variability of the neutron flux. They exclude uncertainty in the J -factor resulting from standard inter-aliquot variability and errors on the K, Ca, Cl correction factors.

5.2. Interpretation of spectra

Mineral ages in high-grade metamorphic terranes are generally interpreted as the time of

Table 1
Hornblende $^{40}\text{Ar}/^{39}\text{Ar}$ isotopic data: sample B114

Temperature (°C)	$^{40}\text{Ar}/$ ^{39}Ar	$^{37}\text{Ar}/$ ^{39}Ar	$^{36}\text{Ar}/$ ^{39}Ar (10^{-3})	$^{38}\text{Ar}/$ ^{39}Ar (10^{-3})	$^{37}\text{Ar}/$ ^{38}Ar	^{39}Ar Cum. (%)	$^{40}\text{Ar}^*$ (%)	$^{40}\text{Ar}^*/$ ^{39}Ar	Ca/K	$^{40}\text{Ar}^*/$ ^{37}Ar	Apparent age ± 2 SD (Ma)
<i>Aliquot (a) Weight = 8.66 mg, J = 0.08564</i>											
700	56.13	0.69	160.22	48.95	14.11	5.78	15.49	8.70	1.38	12.59	1010 \pm 192
775	13.57	0.34	19.42	26.31	12.73	11.99	58.03	7.87	0.67	23.50	930 \pm 140
830	7.95	1.56	3.28	27.89	55.94	22.58	88.64	7.05	3.13	4.52	856 \pm 98
870	7.33	2.94	0.50	38.79	75.69	58.46	99.99	7.35	5.93	2.50	886 \pm 2
900	7.42	2.84	0.00	36.49	77.92	85.39	99.99	7.82	5.70	2.75	929 \pm 48
930	7.29	1.56	0.00	26.95	57.86	92.92	99.99	8.56	3.14	5.49	994 \pm 140
960	7.53	2.07	0.00	28.21	73.36	98.44	99.99	9.19	4.15	4.44	1050 \pm 150
1020	8.72	2.39	2.79	36.06	66.26	99.65	92.13	8.03	4.80	3.36	947 \pm 74
1150	9.87	2.64	0.00	36.08	73.19	99.85	99.99	11.83	5.32	4.48	1270 \pm 256
1450	29.96	2.61	50.71	46.28	56.32	100.00	50.65	15.18	5.26	5.82	1510 \pm 284
<i>Aliquot (b), weight = 5.20 mg, J = 0.08299</i>											
720	9.57	0.21	5.35	16.79	12.80	4.68	83.52	7.99	0.43	37.17	918 \pm 58
800	8.80	1.46	4.09	21.55	67.97	20.56	87.20	7.68	2.94	5.24	895 \pm 14
850	7.90	2.02	0.75	23.81	84.70	33.76	98.61	7.79	4.05	3.86	901 \pm 10
900	7.97	2.94	0.14	28.87	101.82	48.64	99.99	8.12	5.93	2.76	935 \pm 44
950	7.94	3.00	0.35	29.07	103.04	71.45	99.99	7.99	6.03	2.67	924 \pm 6
970	8.06	2.08	0.00	24.51	84.67	78.30	99.99	8.24	4.17	3.97	943 \pm 88
1020	8.04	2.79	0.47	27.77	100.32	90.83	99.99	8.04	5.61	2.89	926 \pm 2
1150	8.34	3.06	0.50	28.87	105.96	99.93	99.99	8.35	6.15	2.73	955 \pm 4

Table 2
Hornblende $^{40}\text{Ar}/^{39}\text{Ar}$ isotopic data: sample B185, weight = 5.82 mg, $J = 0.08564$

Temperature (°C)	$^{40}\text{Ar}/$ ^{39}Ar	$^{37}\text{Ar}/$ ^{39}Ar	$^{36}\text{Ar}/$ ^{39}Ar (10^{-3})	$^{38}\text{Ar}/$ ^{39}Ar (10^{-3})	$^{37}\text{Ar}/$ ^{38}Ar	^{39}Ar Cum. (%)	$^{40}\text{Ar}^*$ (%)	$^{40}\text{Ar}^*/$ ^{39}Ar	Ca/K	$^{40}\text{Ar}^*/$ ^{37}Ar	Apparent age ± 2 SD (Ma)
750	16.22	0.37	26.34	23.81	15.50	0.78	51.93	8.42	0.74	22.82	981 \pm 134
775	22.49	0.41	52.65	27.93	14.55	1.60	30.75	6.91	0.81	17.01	839 \pm 128
800	32.19	0.62	80.34	39.43	15.76	2.54	26.07	8.39	1.24	13.50	978 \pm 126
850	25.11	1.43	59.70	38.72	36.89	4.08	29.94	7.52	2.87	5.26	902 \pm 82
900	11.99	2.35	15.59	41.80	56.15	7.67	62.47	7.49	4.72	3.19	899 \pm 32
925	7.93	3.15	2.72	45.35	69.49	17.61	91.94	7.29	6.35	2.31	880 \pm 10
950	7.40	3.36	1.43	46.19	72.72	43.37	96.97	7.17	6.78	2.14	868 \pm 4
1000	7.33	3.30	1.23	45.29	72.83	87.50	97.50	7.15	6.65	2.17	867 \pm 2
1050	8.24	2.57	3.92	38.11	67.48	90.25	87.76	7.23	5.18	2.81	875 \pm 34
1250	7.49	3.48	1.53	45.23	77.04	99.93	96.50	7.23	7.02	2.08	875 \pm 8
1450	58.48	3.93	96.45	51.21	76.66	100.00	51.38	30.05	7.91	7.65	2310 \pm 808

cooling through the closure temperature for volume diffusion of the parent and radiogenic isotopes (Dodson, 1973). Regional variations of the cooling process can be evaluated by comparing a specific geochronometer at different localities, while the rate of cooling can be estimated by the use of several geochronometers with different closure temperatures. Such an approach allows terranes with variable uplift histories to be identified,

these terranes being usually separated by tectonic boundaries. It has been successfully used to unravel the cooling histories in many complex orogenic belts.

Ideally, amphibole $^{40}\text{Ar}/^{39}\text{Ar}$ dating provides a release spectrum with a concordant plateau age and a similar intercept age on an inverse isotope correlation diagram ($^{39}\text{Ar}/^{40}\text{Ar}$ versus $^{36}\text{Ar}/^{40}\text{Ar}$) with an initial atmospheric $^{36}\text{Ar}/^{40}\text{Ar}$ ratio. The

Table 3

Hornblende $^{40}\text{Ar}/^{39}\text{Ar}$ isotopic data: sample B195, weight = 5.02 mg, $J = 0.08299$

Temperature (°C)	$^{40}\text{Ar}/^{39}\text{Ar}$	$^{37}\text{Ar}/^{39}\text{Ar}$	$^{36}\text{Ar}/^{39}\text{Ar}$ (10^{-3})	$^{38}\text{Ar}/^{39}\text{Ar}$ (10^{-3})	$^{37}\text{Ar}/^{38}\text{Ar}$	^{39}Ar Cum. (%)	$^{40}\text{Ar}^*$ (%)	$^{40}\text{Ar}^*/^{39}\text{Ar}$	Ca/K	$^{40}\text{Ar}^*/^{37}\text{Ar}$	Apparent age ± 2 SD (Ma)
600	371.87	34.55	363.96	754.29	45.80	0.46	71.63	266.37	75.20	7.71	5800 \pm 3160
700	227.61	2.83	379.85	51.87	54.53	2.07	50.82	115.67	5.70	40.90	4270 \pm 1280
800	477.78	—	1129.19	141.61	—	3.05	30.15	144.07	—	—	4620 \pm 1998
870	140.18	1.89	438.60	112.63	16.82	5.91	7.40	10.37	3.80	5.47	1120 \pm 374
920	200.00	2.16	630.67	154.64	13.97	8.24	6.89	13.78	4.34	6.38	1380 \pm 398
1000	217.74	1.62	658.60	152.42	10.62	10.11	10.41	22.66	3.25	14.00	1910 \pm 348
1050	360.00	2.69	1157.33	249.33	10.80	11.99	4.52	16.27	5.43	6.04	1550 \pm 456
1100	162.12	1.52	407.54	82.59	18.37	18.71	25.47	41.29	3.05	27.22	2690 \pm 626
1130	107.53	2.87	20.16	37.58	76.39	20.95	94.50	101.61	5.77	35.39	4060 \pm 1304
1145	170.33	3.34	0.00	—	—	22.05	99.99	291.21	6.73	87.17	5830 \pm 1258
1170	125.78	1.12	350.93	78.88	14.17	23.66	17.14	21.55	2.24	19.28	1850 \pm 406
1200	138.60	1.35	404.65	90.93	14.83	25.82	13.59	18.84	2.70	13.97	1700 \pm 338
1230	92.47	1.75	267.53	74.68	23.48	29.69	14.47	13.38	3.52	7.63	1350 \pm 232
1260	41.74	2.38	108.26	46.52	51.21	41.24	23.54	9.83	4.80	4.12	1080 \pm 88
1280	8.39	2.94	1.70	28.65	102.55	75.60	95.82	8.04	5.93	2.74	928 \pm 16
1300	79.86	2.45	231.94	69.17	35.44	82.83	14.00	11.18	4.94	4.56	1190 \pm 138
1360	97.20	2.87	290.21	82.52	34.75	90.01	11.73	11.40	5.76	3.98	1200 \pm 142
1500	3812.22	55.88	11488.89	2600.67	21.49	100.00	10.95	417.26	5.10	7.47	1710 \pm 348

Table 4

Hornblende $^{40}\text{Ar}/^{39}\text{Ar}$ isotopic data: sample B198, weight = 6.04 mg, $J = 0.08299$

Temperature (°C)	$^{40}\text{Ar}/^{39}\text{Ar}$	$^{37}\text{Ar}/^{39}\text{Ar}$	$^{36}\text{Ar}/^{39}\text{Ar}$ (10^{-3})	$^{38}\text{Ar}/^{39}\text{Ar}$ (10^{-3})	$^{37}\text{Ar}/^{38}\text{Ar}$	^{39}Ar Cum. (%)	$^{40}\text{Ar}^*$ (%)	$^{40}\text{Ar}^*/^{39}\text{Ar}$	Ca/K	$^{40}\text{Ar}^*/^{37}\text{Ar}$	Apparent age ± 2 SD (Ma)
600	626.80	7.46	1515.46	—	—	0.07	28.39	177.94	15.20	23.84	5000 \pm 3140
700	176.52	1.16	495.65	116.52	9.93	0.38	17.36	30.65	2.31	26.50	2280 \pm 4740
750	453.58	—	875.44	357.23	—	0.49	42.75	193.89	—	—	5120 \pm 1552
800	384.72	0.17	1173.61	250.69	0.67	0.57	9.37	36.04	0.34	213.58	2500 \pm 652
840	449.64	0.07	1332.66	263.48	0.28	0.63	12.29	55.24	0.15	740.79	3100 \pm 672
880	460.59	0.48	1385.14	259.01	1.87	0.68	111.27	51.91	0.97	107.46	3010 \pm 770
920	394.34	1.15	1169.81	231.13	4.98	0.74	12.27	48.40	2.31	42.05	2910 \pm 690
980	378.89	1.91	1172.22	245.00	7.80	0.84	8.45	32.00	3.84	16.74	2350 \pm 560
1020	342.42	2.67	1096.97	226.36	11.78	1.03	5.27	18.03	5.37	6.76	1660 \pm 474
1060	217.82	1.92	694.48	162.66	11.83	1.43	5.95	12.96	3.87	6.74	1320 \pm 284
1080	115.73	1.28	338.03	78.40	16.35	1.67	13.73	15.89	2.57	12.40	1520 \pm 378
1200	8.13	3.10	3.14	35.65	86.99	95.55	90.55	7.36	6.24	2.37	875 \pm 20
1260	66.82	2.03	147.40	94.65	21.49	96.44	35.01	23.39	4.08	11.50	1950 \pm 1658
1300	78.60	3.05	232.31	79.04	38.62	97.73	12.67	9.96	6.16	3.26	1090 \pm 102
1350	67.43	3.03	195.77	70.36	43.06	99.47	14.25	9.61	6.11	3.17	1060 \pm 80
1400	492.96	3.09	1431.92	90.61	34.15	99.75	13.90	68.54	6.22	22.15	3400 \pm 1372
1500	1121.55	5.97	3546.96	718.23	8.31	100.00	6.65	74.59	12.10	12.50	4580 \pm 1632

reproducibility of the Ar isotopic composition for consecutive heating steps is the main argument for considering that the released Ar is undisturbed radiogenic ^{40}Ar , generally distributed in highly retentive sites of the crystals. Disturbed age spectra have been commonly reported and interpreted as

evidence for partial loss of radiogenic ^{40}Ar or the presence of extraneous ^{40}Ar [excess Ar; e.g. Harrison and McDougall (1981)]. A number of other analytical and mineralogical phenomena may complicate the interpretation of spectra. Three of them are relevant.

Table 5
Hornblende $^{40}\text{Ar}/^{39}\text{Ar}$ isotopic data: sample B308

Temperature (°C)	$^{40}\text{Ar}/$ ^{39}Ar	$^{37}\text{Ar}/$ ^{39}Ar	$^{36}\text{Ar}/$ ^{39}Ar (10^{-3})	$^{38}\text{Ar}/$ ^{39}Ar (10^{-3})	$^{37}\text{Ar}/$ ^{38}Ar	^{39}Ar Cum. (%)	$^{40}\text{Ar}^*$ (%)	$^{40}\text{Ar}^*/$ ^{39}Ar	Ca/K	$^{40}\text{Ar}^*/$ ^{37}Ar	Apparent age ± 2 SD (Ma)
<i>Aliquot (a) Weight = 6.61 mg, J = 0.08299</i>											
550	55.39	2.02	156.43	64.89	31.07	1.09	16.55	9.17	4.06	4.55	1020.130
600	32.06	1.07	72.98	36.11	29.60	4.87	32.86	10.53	2.13	9.86	1130 \pm 78
700	9.47	1.28	4.76	39.96	34.55	7.98	85.80	8.12	2.56	6.36	931 \pm 24
800	7.61	2.64	0.83	49.55	53.33	48.89	98.62	7.51	5.30	2.84	878 \pm 2
850	7.65	2.80	0.68	50.29	55.70	88.16	99.04	7.57	5.64	5.70	887 \pm 2
900	1.74	0.61	0.00	10.88	56.50	97.55	999.99	2.13	5.81	3.47	1100 \pm 188
950	9.52	3.02	4.24	51.75	58.28	98.32	888.33	8.41	6.09	2.79	963 \pm 86
1100	8.97	2.90	3.04	52.47	55.22	99.94	91.95	8.25	5.84	2.85	945 \pm 30
1150	61.99	2.81	178.15	83.44	33.65	99.98	15.17	9.40	5.64	3.35	1040 \pm 138
<i>Aliquot (b) weight = 7.27 mg, J factor = 0.08564</i>											
620	397.22	3.72	1298.61	227.78	16.34	1.32	3.51	13.96	7.53	3.75	1430 \pm 680
670	18.82	0.88	35.29	24.03	36.71	3.59	44.29	8.34	1.77	9.45	974 \pm 50
720	25.60	0.26	63.65	31.57	8.32	5.82	26.20	6.71	0.53	25.52	819 \pm 44
770	26.40	1.12	64.53	37.14	30.24	9.46	27.99	7.39	2.25	6.58	888 \pm 118
820	8.88	2.82	6.19	43.38	65.00	25.99	81.07	7.20	5.69	2.55	871 \pm 22
870	7.33	3.23	1.24	47.06	68.65	65.61	97.53	7.15	6.52	2.21	868 \pm 6
920	7.76	3.23	1.95	46.64	69.18	88.56	94.86	7.36	6.49	2.28	885 \pm 12
970	8.99	3.53	6.27	48.05	73.52	95.01	80.92	7.28	7.12	2.06	881 \pm 12
1056	10.85	3.88	11.86	49.94	77.69	98.06	69.55	7.55	7.82	1.95	906 \pm 28
1146	7.99	3.56	1.19	49.19	72.31	99.93	97.96	7.83	7.17	2.20	931 \pm 20
1500	28.88	11.29	2.37	31.07	363.47	100.00	99.61	28.76	23.20	2.55	2280 \pm 84

Table 6
Hornblende $^{40}\text{Ar}/^{39}\text{Ar}$ isotopic data: sample B613, weight = 5.44 mg, $J = 0.08564$

Temperature (°C)	$^{40}\text{Ar}/$ ^{39}Ar	$^{37}\text{Ar}/$ ^{39}Ar	$^{36}\text{Ar}/$ ^{39}Ar (10^{-3})	$^{38}\text{Ar}/$ ^{39}Ar (10^{-3})	$^{37}\text{Ar}/$ ^{38}Ar	^{39}Ar Cum. (%)	$^{40}\text{Ar}^*$ (%)	$^{40}\text{Ar}^*/$ ^{39}Ar	Ca/K	$^{40}\text{Ar}^*/$ ^{37}Ar	Apparent age ± 2 SD (Ma)
700	332.06	5.27	1099.24	160.31	32.86	0.30	1.95	6.49	10.70	1.23	805 \pm 1190
775	17.41	0.47	33.29	25.80	18.10	1.92	43.37	7.55	0.94	16.17	903 \pm 78
202	26.84	0.34	70.06	31.69	10.73	3.93	22.74	6.10	0.68	17.94	761 \pm 60
850	8.94	2.46	6.99	38.44	64.02	19.93	78.57	7.02	4.95	2.85	854 \pm 10
875	7.36	3.01	1.40	40.61	74.03	57.38	96.71	7.12	6.05	2.37	863 \pm 4
900	7.44	3.12	1.65	40.76	76.49	84.38	95.48	7.10	6.27	2.28	861 \pm 4
960	8.17	3.12	3.93	40.33	77.27	91.19	87.76	7.17	6.28	2.30	869 \pm 16
1050	8.97	3.61	6.03	42.86	84.29	98.10	82.23	7.37	7.29	2.04	889 \pm 14
1200	9.02	3.99	3.60	41.89	95.20	99.96	90.54	8.17	8.05	2.05	962 \pm 60
1500	170.61	3.67	322.68	91.69	40.07	100.00	44.38	75.72	7.42	20.61	3640 \pm 702

- (1) Laboratory heating causes dehydroxylation and structural changes in the minerals; the release of Ar from the mineral during the experiment is thus more complex than volume diffusion and may occur over a narrow temperature range (Lee et al., 1991).
- (2) Small scale inhomogeneity of the concentrates, for example, a mixture of different generations

of amphibole with different thermal retentivity or presence of (micro)inclusions of K-rich, less retentive, younger minerals in amphibole, possibly result in perturbed spectra (Wartho, 1995). Secondary minerals may crystallize or re-crystallize close to or below the closure temperature. In this situation, ages reflect crystallization rather than cooling.

Table 7

Hornblende $^{40}\text{Ar}/^{39}\text{Ar}$ isotopic data: sample B630

Temperature (°C)	$^{40}\text{Ar}/$ ^{39}Ar	$^{37}\text{Ar}/$ ^{39}Ar	$^{36}\text{Ar}/$ ^{39}Ar (10^{-3})	$^{38}\text{Ar}/$ ^{39}Ar (10^{-3})	$^{37}\text{Ar}/$ ^{38}Ar	^{39}Ar Cum. (%)	$^{40}\text{Ar}^*$ (%)	$^{40}\text{Ar}^*/$ ^{39}Ar	Ca/K	$^{40}\text{Ar}^*/$ ^{37}Ar	Apparent age ± 2 SD (Ma)
<i>Aliquot (a) Weight = 6.90 mg, J factor = 0.08564</i>											
600	8.43	0.41	21.16	12.05	34.37	2.46	26.19	2.21	0.83	5.33	313 ± 84
650	9.26	0.62	25.12	12.49	49.82	4.46	20.20	1.87	1.24	3.01	269 ± 124
700	20.19	0.90	55.14	26.38	34.15	5.42	19.58	3.95	1.81	4.39	528 ± 170
750	40.10	0.71	127.35	39.43	18.04	5.97	5.86	2.35	1.43	3.30	331 ± 434
830	80.51	4.12	255.59	96.96	42.50	6.54	6.55	5.27	8.34	1.28	678 ± 238
850	60.38	8.58	182.31	54.23	158.16	6.78	11.34	6.85	17.50	0.80	846 ± 546
870	138.97	10.72	430.77	110.77	96.76	6.96	8.60	11.95	21.90	1.11	1300 ± 428
900	143.38	9.71	459.56	105.51	91.99	7.21	5.41	7.76	19.90	0.80	936 ± 524
960	52.65	1.12	145.17	45.17	24.76	7.50	18.64	9.81	2.24	8.77	1100 ± 252
990	32.54	0.47	76.72	30.42	15.30	7.85	30.24	9.84	0.93	21.14	1100 ± 288
1040	20.72	0.45	42.46	24.64	18.29	8.49	39.30	8.14	0.90	18.07	955 ± 130
1100	24.68	0.61	57.06	27.91	22.02	9.28	31.59	7.80	1.23	12.68	924 ± 126
1140	8.02	3.33	4.00	46.71	71.37	99.95	87.50	7.02	6.73	2.11	855 ± 2
1180	201.41	2.84	508.83	187.99	15.13	99.97	25.44	51.24	5.72	18.01	3040 ± 1276
1250	343.42	2.64	1042.70	231.323	11.42	100.00	10.03	34.45	5.31	13.05	2490 ± 1826
<i>Aliquot (b), weight = 7.58 mg, J factor = 0.08564</i>											
800	33.33	1.18	90.54	35.44	33.23	8.53	19.87	6.62	2.37	5.63	812 ± 78
850	21.36	1.03	46.94	39.80	25.90	11.16	35.19	7.52	2.07	7.29	898 ± 52
950	7.49	2.68	1.69	50.86	52.73	79.04	95.41	7.15	5.41	2.67	865 ± 2
1000	7.65	2.81	1.81	50.90	55.19	87.53	95.03	7.27	5.66	2.59	877 ± 8
1040	7.80	2.91	2.22	51.65	56.37	91.07	93.51	7.29	5.89	2.50	888 ± 18
1090	7.76	2.94	1.26	51.26	57.07	94.51	97.32	7.55	5.91	2.57	904 ± 16
1120	8.40	2.88	0.91	52.03	55.29	96.19	98.73	8.29	5.80	2.88	972 ± 28
1160	8.42	3.04	1.02	51.15	59.49	97.44	98.29	8.27	6.14	2.72	975 ± 42
1200	8.50	3.10	1.04	51.50	60.15	98.63	98.23	8.35	6.25	2.69	980 ± 38
1400	9.02	2.96	1.46	54.05	54.78	100.00	97.10	8.76	5.96	2.96	1010 ± 64

Microtextural features like fractures, dislocations, inclusions, exsolution lamellae subdivide the grains into subdomains with possible distinct diffusion properties and represent channels for Ar escape or introduction of excess Ar (Kelley and Turner, 1991; Lee, 1995).

In order to evaluate the data, $^{40}\text{Ar}/^{39}\text{Ar}$ age spectra, Ca/K spectra as well as inverse isotope correlation plots are presented for each fraction in Fig. 3. Although hand-picking was carefully performed, differences in ages and shape of spectra for different aliquots of some samples were observed; they could be related to inhomogeneity at sub-sampling level (e.g. von Blanckenburg and Villa, 1988). For this reason, regional averages of $^{40}\text{Ar}/^{39}\text{Ar}$ ages were calculated in two steps by referring first to the aliquots for each sample and

then to the different samples (errors encompass maximum and minimum sample averages). On the other hand, the heating procedure adopted in this study did not allow the definition of a good plateau age for a number of concentrates degassing over a narrow temperature interval. Heating with smaller temperature increments could have produced more smooth spectra, but may just as well have created artificial plateaus which do not correspond to the *in situ* distribution of Ar. For most fractions, the good alignment of points on the inverse isotope correlation plot and the concordance between the Ca/K ratios derived from the $^{40}\text{Ar}/^{39}\text{Ar}$ heating experiments and those obtained by microprobe (Bingen, 1988) suggest that most spectra with a few steps provide representative hornblende ages.

Table 8
Hornblende $^{40}\text{Ar}/^{39}\text{Ar}$ isotopic data: sample B671

Temperature (°C)	$^{40}\text{Ar}/$ ^{39}Ar	$^{37}\text{Ar}/$ ^{39}Ar	$^{36}\text{Ar}/$ $^{39}\text{Ar} (10^{-3})$	$^{38}\text{Ar}/$ $^{39}\text{Ar} (10^{-3})$	$^{37}\text{Ar}/$ ^{38}Ar	^{39}Ar Cum. (%)	$^{40}\text{Ar}^*$ (%)	$^{40}\text{Ar}^*/$ ^{39}Ar	Ca/K	$^{40}\text{Ar}^*/$ ^{37}Ar	Apparent age ± 2 SD (Ma)
<i>Aliquot (a) Weight = 7.66 mg, J factor = 0.08564</i>											
600	176.85	0.93	569.13	1141.31	8.10	5.42	4.87	8.62	1.85	9.31	998 \pm 128
700	124.14	1.03	382.76	82.41	12.45	15.53	8.89	11.03	2.06	10.76	1210 \pm 156
800	261.64	0.46	859.20	178.49	2.59	23.39	2.59	6.78	0.92	14.68	827 \pm 216
850	26.89	0.63	22.89	23.94	26.45	24.96	75.00	20.17	1.27	31.84	1810 \pm 442
900	14.89	1.59	0.00	36.25	43.75	27.65	99.99	15.92	3.18	10.04	1560 \pm 352
950	7.76	2.31	2.01	39.12	59.13	53.27	93.86	7.28	4.66	3.15	880 \pm 52
980	7.13	2.24	1.03	37.07	60.47	83.59	97.58	6.95	4.50	3.10	846 \pm 24
1000	6.67	1.60	3.21	32.05	49.80	97.18	87.50	5.83	3.21	3.65	734 \pm 64
1080	16.96	2.31	22.84	37.12	62.16	99.79	60.95	10.33	4.65	4.48	1150 \pm 304
<i>Aliquot (b) Weight = 5.90 mg, J factor = 0.08564</i>											
700	152.37	1.97	451.55	97.11	20.25	4.66	12.21	18.60	3.95	9.45	1720 \pm 226
800	67.18	1.83	193.38	69.97	26.11	8.44	14.81	9.95	3.68	5.45	112 \pm 410
900	7.96	2.41	2.18	40.98	58.90	80.94	93.50	7.44	4.86	3.08	893 \pm 14
920	9.39	2.50	0.00	44.66	55.98	84.90	99.99	10.85	5.00	4.34	1190 \pm 234
940	9.36	2.59	0.00	44.20	58.69	88.38	99.99	11.49	5.22	4.43	1240 \pm 234
970	9.28	2.47	5.20	41.76	59.15	92.47	84.90	7.88	4.97	3.19	934 \pm 20
1010	8.96	2.44	3.89	41.00	59.51	96.48	88.62	7.94	4.91	3.25	939 \pm 20
1060	10.19	2.40	7.18	41.51	57.81	98.76	80.41	8.20	4.84	3.42	964 \pm 36
1140	19.53	2.35	33.29	46.94	50.13	99.45	50.00	9.76	4.73	4.15	1100 \pm 116
1300	38.26	2.22	93.18	55.38	40.08	99.97	28.51	10.91	4.46	4.91	1200 \pm 146

Table 9
Hornblende $^{40}\text{Ar}/^{39}\text{Ar}$ isotopic data: sample D84/8, weight = 10.15 mg, J factor = 0.08564

Temperature (°C)	$^{40}\text{Ar}/$ ^{39}Ar	$^{37}\text{Ar}/$ ^{39}Ar	$^{36}\text{Ar}/$ $^{39}\text{Ar} (10^{-3})$	$^{38}\text{Ar}/$ $^{39}\text{Ar} (10^{-3})$	$^{37}\text{Ar}/$ ^{38}Ar	^{39}Ar Cum. (%)	$^{40}\text{Ar}^*$ (%)	$^{40}\text{Ar}^*/$ ^{39}Ar	Ca/K	$^{40}\text{Ar}^*/$ ^{37}Ar	Apparent age ± 2 SD (Ma)
800	34.56	0.69	87.96	46.60	14.79	4.17	24.89	8.60	1.38	12.48	997 \pm 36
850	15.15	1.68	23.23	64.38	26.12	11.40	55.11	8.35	3.39	4.97	976 \pm 16
890	9.49	2.23	2.82	72.00	31.03	25.40	92.17	8.74	4.48	3.91	1010 \pm 8
940	9.04	2.33	0.84	73.27	31.85	84.37	98.50	8.90	4.69	3.81	1030 \pm 2
980	9.44	2.33	2.19	68.09	34.15	89.63	94.52	8.92	4.66	3.84	1030 \pm 12
1050	9.76	2.63	3.55	71.05	37.04	92.67	90.57	8.84	5.29	3.36	1020 \pm 26
1120	9.71	2.88	1.10	73.38	39.29	95.14	98.33	9.55	5.80	3.31	1080 \pm 18
1250	9.40	2.88	1.30	73.53	39.18	99.91	97.50	9.16	5.81	3.18	1050 \pm 10

6. Results

6.1. Results from the Rogaland–Vest Agder terrane

Nine samples were analysed in Rogaland–Vest Agder. For the Hidderskog metacharnockitic augen gneiss (Gjerstad suite), amphibole was purified in sample B308 which gives a zircon U–Pb crystallization age of 1159 ± 5 Ma (Zhou et al., 1995). Two amphibole splits yield slightly different $^{40}\text{Ar}/^{39}\text{Ar}$ spectra. For aliquot (a), two single-step

ages of 878 ± 2 Ma (41% of released ^{39}Ar) and 887 ± 2 Ma (39% of released ^{39}Ar) are relevant and similar to the intercept age of 878 ± 2 Ma. Aliquot (b) yields a three-step age of 875 ± 9 Ma [69% of released ^{39}Ar , Fig. 3(E)] equivalent to the intercept age (872 ± 5 Ma). The Ca/K ratios, corresponding to the heating steps releasing most of the ^{39}Ar , are slightly different for the two aliquots although this may be expected considering the small size of the samples.

Hornblende was separated from five samples of

Table 10

Hornblende $^{40}\text{Ar}/^{39}\text{Ar}$ isotopic data: sample P1158, weight = 0.5598 g, $J = 0.01974$

Temperature (°C)	$^{40}\text{Ar}/^{39}\text{Ar}$	$^{37}\text{Ar}/^{39}\text{Ar}$	$^{36}\text{Ar}/^{39}\text{Ar}$ (10^{-3})	^{39}Ar Cum. (%)	$^{40}\text{Ar}^*$ (%)	$^{40}\text{Ar}^*/^{39}\text{Ar}$	$^{40}\text{Ar}^*/^{37}\text{Ar}$	Ca/K	Apparent age ± 2 SD (Ma)
550	5181.72	7.33	524.27	0.06	97.00	5026.27	682.34	14.44	8312 \pm 24
700	1760.75	6.63	361.89	0.20	94.00	1655.11	248.37	13.07	6313 \pm 26
750	442.92	6.96	171.96	0.29	88.70	392.87	56.20	13.71	1621 \pm 16
840	88.70	5.39	52.04	0.74	83.20	73.80	13.65	10.60	944 \pm 14
900	45.73	4.42	4.77	9.45	97.10	44.40	10.01	8.69	922 \pm 12
930	34.11	4.39	2.42	43.60	99.00	33.77	7.66	8.64	917 \pm 8
940	33.81	4.39	2.04	75.37	99.30	33.58	7.63	8.63	915 \pm 8
950	36.13	4.38	10.20	76.64	92.70	33.49	7.62	8.62	920 \pm 8
960	34.71	4.41	5.43	77.27	96.60	33.53	7.58	8.67	916 \pm 8
1000	34.69	4.38	4.68	78.12	97.10	33.69	7.66	8.62	920 \pm 8
1020	33.95	4.39	2.61	80.17	98.80	33.55	7.61	8.64	917 \pm 8
1030	33.89	4.39	2.12	86.21	99.20	33.62	7.63	8.63	919 \pm 8
1050	3390	4.39	2.35	91.73	98.40	33.60	7.63	8.64	918 \pm 8
Fusion	32.61	5.14	3.36	100.00	98.10	32.09	6.23	10.11	919 \pm 8

Table 11

Hornblende $^{40}\text{Ar}/^{39}\text{Ar}$ isotopic data: sample HA54, weight = 0.4799 g, $J = 0.01953$

Temperature (°C)	$^{40}\text{Ar}/^{39}\text{Ar}$	$^{37}\text{Ar}/^{39}\text{Ar}$	$^{36}\text{Ar}/^{39}\text{Ar}$ (10^{-3})	^{39}Ar Cum. (%)	$^{40}\text{Ar}^*$ (%)	$^{40}\text{Ar}^*/^{39}\text{Ar}$	$^{40}\text{Ar}^*/^{37}\text{Ar}$	Ca/K	Apparent age ± 2 SD (Ma)
550	175.10	5.10	369.47	0.03	37.90	66.36	13.01	10.00	1500 \pm 78
650	216.35	5.72	231.24	0.05	68.60	148.42	25.94	11.22	2456 \pm 38
750	247.66	5.32	125.09	0.09	85.30	211.25	39.72	10.43	2948 \pm 26
850	151.90	4.76	115.85	0.19	77.20	117.26	24.64	9.33	2157 \pm 24
900	82.60	4.33	104.09	0.26	63.20	52.21	12.04	8.50	1268 \pm 26
930	58.10	3.64	59.18	0.36	70.40	40.90	11.24	7.13	1060 \pm 36
960	42.85	3.14	21.98	0.69	85.40	36.59	11.65	6.16	973 \pm 9
980	40.18	3.07	16.04	0.96	88.80	35.68	11.62	6.02	954 \pm 8
1010	36.16	2.93	7.08	1.96	94.90	34.31	11.69	5.75	925 \pm 8
1030	34.33	2.90	2.70	6.26	98.40	33.78	11.66	5.68	913 \pm 7
1050	33.89	2.89	1.83	12.45	99.10	33.58	11.62	5.67	910 \pm 8
1060	33.79	2.88	1.57	26.41	99.30	33.56	11.66	5.64	909 \pm 7
1070	33.93	2.88	2.01	30.31	98.90	33.56	111.67	5.64	909 \pm 8
1080	33.68	2.88	1.32	49.44	99.50	33.51	11.64	5.64	908 \pm 8
1090	33.73	2.87	1.36	59.33	99.50	33.56	11.68	5.63	909 \pm 8
1100	33.73	2.87	1.48	64.90	99.40	33.53	11.67	5.63	908 \pm 8
1110	33.69	2.88	1.41	74.32	99.50	33.52	11.63	5.65	908 \pm 8
Fusion	33.69	2.95	2.33	100.00	98.37	33344.01	1135.16	5.78	909 \pm 8

different augen gneiss bodies of the 1.05 Ga Feda suite (Fig. 1). Sample B630 is in the amphibolite-facies domain, north of Mandal. Samples B185 and B114 are situated to the west of the Cpx-in isograd while samples B198 and B195 are in the granulite-facies domain, B195 being the closest (3 km) to the Rogaland Igneous Complex. No secondary alteration of hornblende is observed

petrographically except in sample B630 where chlorite locally occurs in patches or fractures (Appendix A). The two amphibole aliquots of sample B630 [Fig. 3(G)] give a single-step age of 855 ± 2 Ma and a four-step age of 868 ± 4 Ma (91 and 83% of released ^{39}Ar). For aliquot (b), the isotope correlation plot yields an older intercept age of 894 ± 7 Ma compared to 853 ± 3 Ma for

Table 12

Hornblende $^{40}\text{Ar}/^{39}\text{Ar}$ isotopic data: sample ROG43, weight = 0.4350 g, $J = 0.01965$

Temperature (°C)	$^{40}\text{Ar}/$ ^{39}Ar	$^{37}\text{Ar}/$ ^{39}Ar	$^{36}\text{Ar}/$ ^{39}Ar (10^{-3})	^{39}Ar Cum. (%)	$^{40}\text{Ar}^*$ (%)	$^{40}\text{Ar}^*/$ ^{39}Ar	$^{40}\text{Ar}^*/$ ^{37}Ar	Ca/K	Apparent age ± 2 SD (Ma)
550	552.41	4.82	111.40	0.15	93.80	490.02	101.68	9.45	4264 \pm 24
650	737.46	3.42	52.58	0.44	97.90	721.98	211.21	6.70	4909 \pm 26
750	314.22	1.47	26.76	0.88	97.50	306.37	208.06	2.89	3516 \pm 16
840	178.32	1.96	24.46	1.26	96.00	171.19	87.50	3.84	2658 \pm 14
900	88.68	2.31	14.81	1.82	95.30	84.51	36.54	4.53	1765 \pm 12
940	46.91	2.85	3.99	5.33	98.00	45.97	16.12	5.59	1161 \pm 8
970	42.00	2.95	2.29	13.00	99.00	41.58	14.10	5.78	1077 \pm 8
980	40.41	2.97	1.90	16.55	99.20	40.09	13.49	5.82	1048 \pm 8
990	39.67	2.97	1.97	21.75	99.10	39.31	13.24	5.82	1033 \pm 8
1000	38.46	2.98	1.74	26.26	99.30	38.19	12.83	5.84	10110 \pm 8
1010	37.81	2.99	1.50	31.49	99.50	37.62	12.59	5.86	998 \pm 8
1020	39.00	3.00	1.37	40.37	99.60	38.85	12.95	5.88	1023 \pm 8
1030	40.80	2.99	1.21	55.06	99.70	40.68	13.60	5.86	1060 \pm 8
1040	41.23	2.99	1.40	61.08	99.60	41.07	13.72	5.87	1067 \pm 8
1050	40.83	2.98	1.36	79.23	99.60	40.67	13.63	5.85	1059 \pm 8
1060	40.88	2.99	1.75	81.28	99.30	40.59	13.56	5.87	1058 \pm 8
Fusion	40.78	3.01	1.59	100.00	99.40	40.54	13.49	5.89	1057 \pm 8

Table 13

Summary of new hornblende $^{40}\text{Ar}/^{39}\text{Ar}$ ages and published U–Pb ages in the same samples

Terrane	Sample	$^{40}\text{Ar}/^{39}\text{Ar}$ age (Ma $\pm 2\sigma$)			U–Pb age	
		Plateau (or near-plateau)	Single or two-steps (*)	Inverse isochron	Titanite	Zircon
<i>Rogaland–Vest Agder</i>						
Opx-in zone	B195	Feda suite		928 \pm 16	930 \pm 17	
	B198	Feda suite		875 \pm 20	869 \pm 10	920 \pm 4
Cpx-in zone	HA54	Amphibolite	910 \pm 8		902 \pm 2	
	ROG43	Amphibolite	1059 \pm 8	998 \pm 8	928 \pm 3	
	B114(a)	Feda suite		904 \pm 22*	919 \pm 52	918 \pm 2
	B114(b)		930 \pm 24		898 \pm 8	
	B185	Feda suite		867 \pm 2*	868 \pm 2	925 \pm 13
Amphibolite-facies	PI158	Amphibolite	918 \pm 8			
	B308(a)	Gjerstad suite		878 \pm 2 887 \pm 2	878 \pm 2	1159 \pm 5
	B308(b)		875 \pm 9 (three steps)		872 \pm 5	
	B630(a)	Feda suite		855 \pm 2	853 \pm 3	919 \pm 4
	B630(b)		868 \pm 4 (four steps)		894 \pm 7	
<i>Telemark</i>						
	B613	Fennefoss	864 \pm 8		863 \pm 2	
	B671(a)	Gjerstad suite		861 \pm 36*	840 \pm 20	
	B671(b)			893 \pm 14	911 \pm 10	
<i>Bamble</i>						
	D84/8	Gjerstad suite		1030 \pm 4*	1029 \pm 3	

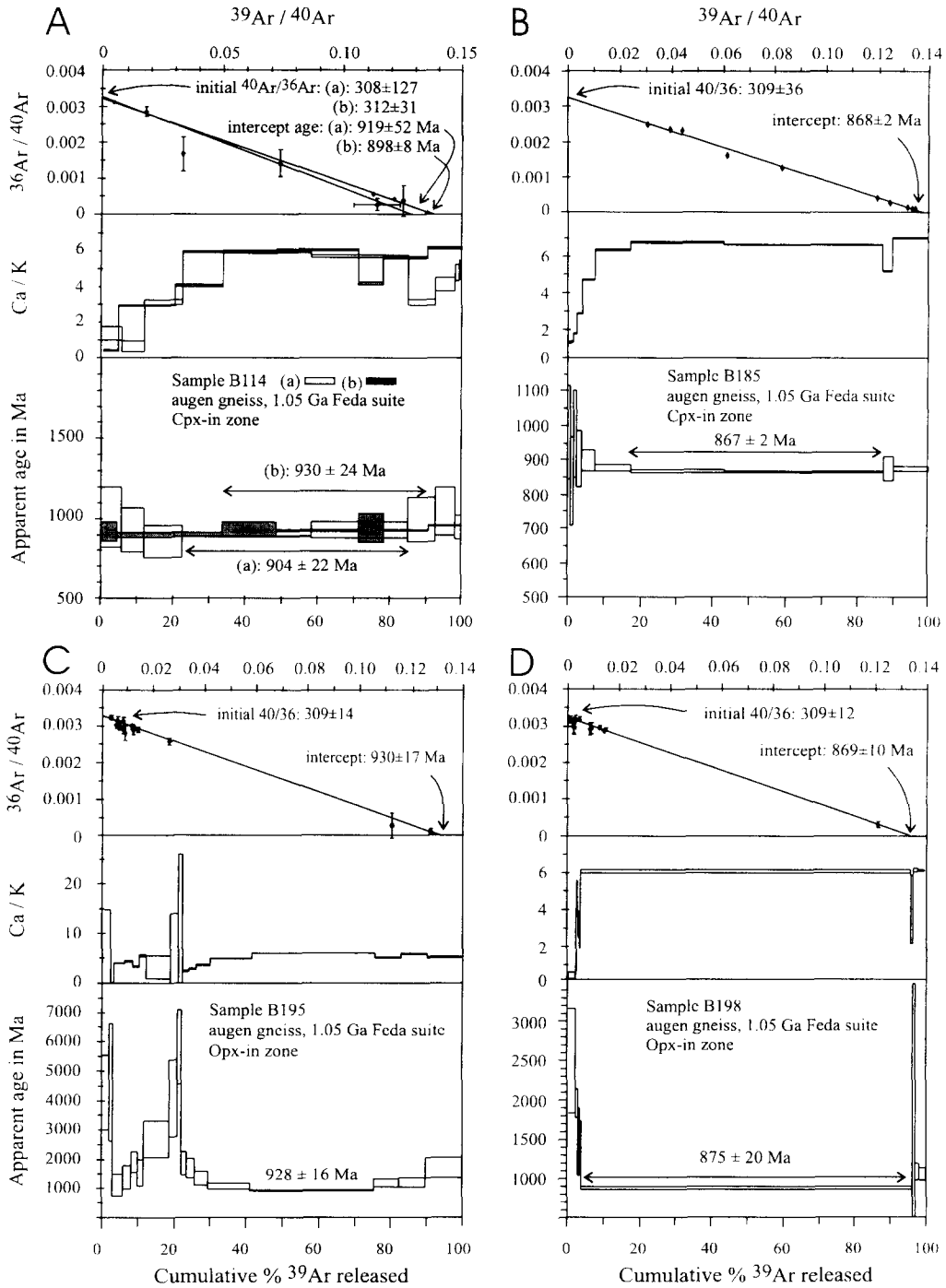


Fig. 3. $^{40}\text{Ar} / ^{39}\text{Ar}$ age spectra, Ca/K spectra and inverse isotope correlation plots of hornblende separates from augen gneiss and amphibolite samples of Rogaland–Vest Agder, Telemark and Bamble terranes (inverse isotope correlation plot for sample P1158 is omitted due to scatter).

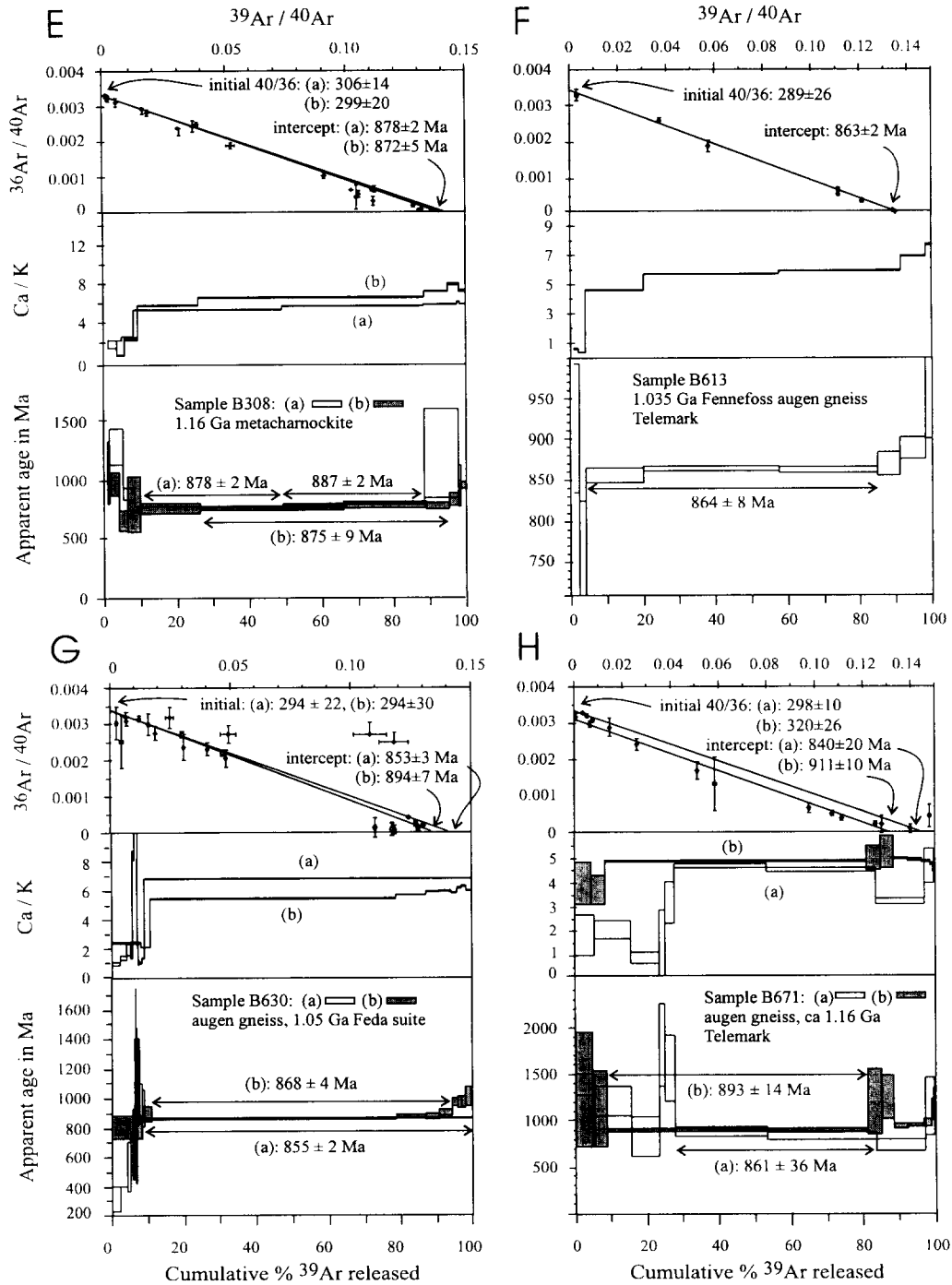


Fig. 3. (continued)

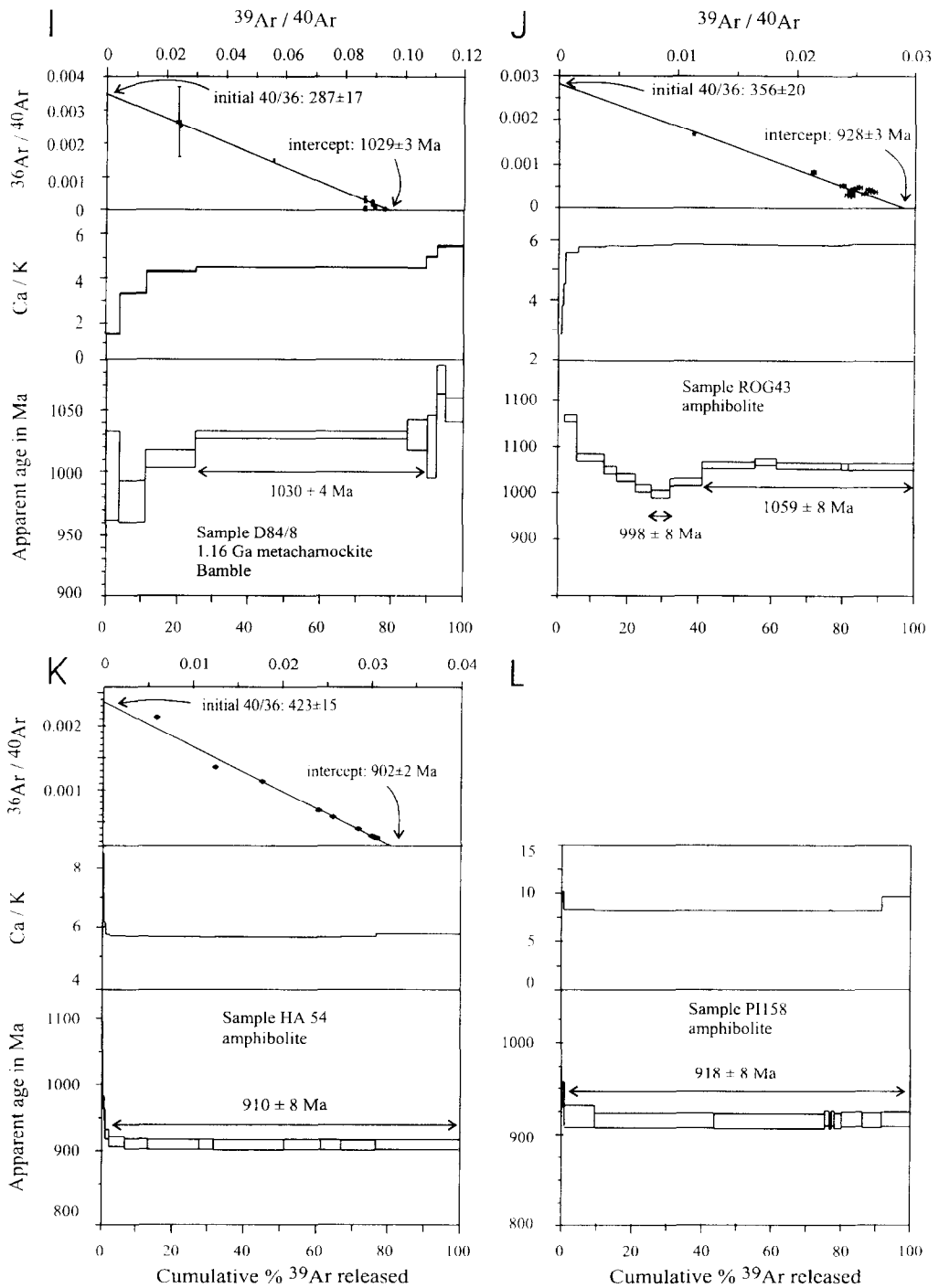


Fig. 3. (continued)

aliquot (a). Samples B185 (west of the Cpx-in isograd) and B198 (west of the Opx-in isograd) yielded similar ages: a two-step age at 867 ± 2 Ma (70% of released ^{39}Ar) for B185 [Fig. 3(B)] and a single-step at 875 ± 20 Ma (93% of ^{39}Ar released) for B198 [Fig. 3(D)]. Impurities degas at low temperatures for both samples, as shown by low Ca/K ratios. Their influence on subsequent steps with high Ca/K ratio, corresponding to hornblende outgassing, is probably limited. Intercept ages are the same for both samples (869 ± 10 and 868 ± 2 Ma). Samples B114 and B195 give significantly older ages. The first split of B114 has a disturbed age spectrum with two large steps at 904 ± 22 Ma (63% of released ^{39}Ar). The isochron age is imprecise (919 ± 52 Ma). The second split yields a plateau age of 930 ± 24 Ma (57% of released ^{39}Ar) and a 898 ± 8 Ma isochron age. The somewhat variable Ca/K ratio points to lack of purity [Fig. 3(A)]. Sample B195 yields a discordant age spectra, with a rough stepwise age increase at low temperature and a saddle-shaped pattern at higher temperature [Fig. 3(C)]. The only step corresponding to important Ar release (34% of released ^{39}Ar) and to a hornblende-like Ca/K ratio (5.9) yields an age of 928 ± 16 Ma while the whole spectrum gives an intercept age of 930 ± 17 Ma on an inverse isochron plot.

Samples ROG43 and HA54 (west of the Opx-in isograd) and PI158 (west of the Cpx-in isograd) are amphibolites. ROG43 [described in Wielens et al. (1981)] is poor in pyroxene but rich in biotite and probably displays limited M2 overprinting. In HA54, a hornblende + biotite + two pyroxenes association (M1) is clearly replaced, in some centimetre-sized patches, by a two pyroxenes dry association (M2). PI158 presents a M2 Cpx-rich biotite-free association. Hornblende displays an homogeneous brown to olive-green colour and is free of alteration in these samples. Hornblendes from PI158 and HA54 yield plateau ages of 918 ± 8 Ma [91% of released ^{39}Ar ; Fig. 3(L)] and 910 ± 8 Ma [98% of ^{39}Ar released; Fig. 3(K)] whereas ROG43 displays an irregular age spectrum with a minimum apparent age of 998 ± 8 Ma at the bottom of a saddle-shaped profile [Fig. 3(J)]. Starting from a release temperature of 1030°C , the profile equilibrates into a plateau with an apparent age of

1059 ± 8 Ma. The intercept age in the isotope correlation plots is 928 ± 3 Ma for ROG43, and 902 ± 2 Ma for HA54. In both cases, high initial $^{40}\text{Ar}/^{36}\text{Ar}$ ratios point to excess Ar; the intercept age is thus preferred for geological interpretation.

6.2. Results from the Telemark terrane

Two samples from S. Telemark were analysed. The pink augen gneiss near Søgne belongs to a group of four large bodies of the 1.19–1.15 Ga Gjerstad suite, situated to the NW of Kristiansand (Bingen and van Breemen, 1998). Two amphibole splits from sample B671 yield discordant age spectra [Fig. 3(H)]. Aliquot (a) gives a two-step apparent age of 861 ± 36 Ma (56% of released ^{39}Ar) and an intercept age of 840 ± 20 Ma, slightly younger but equivalent within the limit of error. The variations in the apparent Ca/K ratio during heating suggest the presence of impurity inclusions. Aliquot (b) yields a saddle-shaped spectrum with a lowest single-step age of 893 ± 14 Ma (73% released ^{39}Ar) and an older intercept age of 911 ± 10 Ma.

Sample B613 of the Fennefoss augen gneiss gives a concordant plateau age of 864 ± 8 Ma [71% of released ^{39}Ar ; Fig. 3(F)]. The excess Ar released in the last steps is related either to impurities or to non-K-bearing sites, as reflected by the high Ca/K values. The intercept age, 863 ± 2 Ma, is equivalent to the plateau age.

6.3. Results from the Bamble terrane

One sample was analysed from Bamble: it comes from the central part of the Hovdefjell metacharnockitic augen gneiss, situated in the hanging wall of the Kristiansand–Porsgrunn shear zone (Fig. 1). Petrologically, this unit is similar to the Gjerstad augen gneiss situated in the footwall of the shear zone. Hornblende from sample D84/8 yields a two-step apparent age of 1030 ± 4 Ma [Fig. 3(I)], equivalent to the intercept age of 1029 ± 3 Ma. These two steps account for 64% of ^{39}Ar released from a single phase as reflected by the similarity of their Ca/K ratios. The three first steps, with abnormally low apparent ages have corresponding low Ca/K values.

7. Discussion

7.1. Mineral ages in Rogaland–Vest Agder and S. Telemark

A large data-set of published mineral ages is available in the high-grade domains of Rogaland–Vest Agder and Telemark (Fig. 4). Titanite U–Pb ages in 12 samples of the Feda suite (including samples B198, B185, B114, B630 of this study) range from 927 to 915 Ma with a weighted average of 918 ± 2 Ma [Fig. 1(A); Bingen and van Breemen (1996)]. Two titanite U–Pb analyses are available in Telemark (Heaman and Smalley, 1994; Bingen and van Breemen, in press); they define ages of 913 and 901 ± 7 Ma, which are similar to or slightly younger than in Rogaland–Vest Agder. Internal Rb–Sr isochrons in one amphibolite-facies augen gneiss (Bingen et al., 1990) and in one post-kinematic charnockite (Maijer et al., 1994) yield ages of 871 ± 35 and 896 ± 13 Ma. Ten K-feldspar megacrysts (≥ 1 cm) from amphibolite- to granulite-facies augen gneiss samples (Feda suite) define a good linear array in the $^{87}\text{Sr}/^{86}\text{Sr}$ versus $^{87}\text{Rb}/^{86}\text{Sr}$ diagram. This array is compatible with the closure of the Rb–Sr system at 870 ± 22 Ma (Bingen et al., 1990). Biotite–whole-rock Rb–Sr ages in ten samples of various gneisses situated outside the Caledonian green biotite-in isograd in Rogaland–Vest Agder range from 895 to 853 Ma

with an average value of 870 Ma and biotite K–Ar ages in the same sample set range from 878 to 853 Ma [one outlier value at 940 Ma; Verschure et al. (1980); Wielens et al. (1981)]. In S. Telemark, two biotite–whole-rock Rb–Sr ages from the Høvringsvatn plutonic complex are available: the one at 929 ± 20 Ma is equivalent to the intrusion of the complex and the other at 874 ± 28 Ma is significantly younger. $^{40}\text{Ar}/^{39}\text{Ar}$ release spectra of plagioclase from anorthosite samples of the Rogaland Complex point to a closure event at ca 750 Ma (Boven et al., 1996; Boven et al., submitted).

Hornblende K–Ar apparent ages from 15 samples of various mafic and felsic gneisses, sampled mainly to the west of the Cpx-in isograd, range from 972 to 937 Ma with one outlier (sample ROG43) at 1171 Ma (Wielens et al., 1981). Most of these high apparent ages probably result from excess Ar incorporation. The hornblende $^{40}\text{Ar}/^{39}\text{Ar}$ ages obtained in this study are significantly younger (Table 1313). They define a bimodal age distribution [Fig. 1(B), Fig. 4].

(1) Two gneiss (B114, B195) and two amphibolite samples (HA54 and PI158) situated to the west of the Cpx-in isograd and close (≤ 10 km) to the Rogaland Igneous Complex, yield ages between 930 and 902 Ma with an average value of $916 \pm 12/-14$ Ma. The intercept age of sample ROG43, 928 ± 3 Ma, is in the same

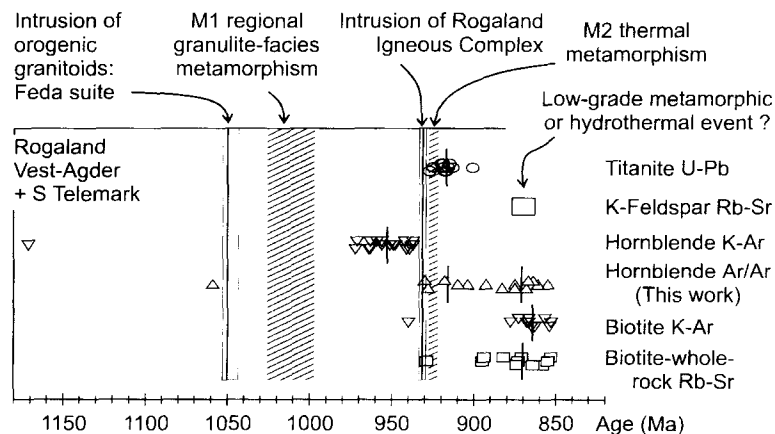


Fig. 4. Compilation of mineral ages in Rogaland–Vest Agder and S. Telemark with average values (vertical bars). Sample ROG43 displays abnormally old biotite and hornblende K–Ar and $^{40}\text{Ar}/^{39}\text{Ar}$ ages probably reflecting excess Ar. References for data in text.

range; it was nevertheless not included in the average calculation because of the significant amount of excess Ar in this sample. The $916 \pm 12 / -14$ Ma average age is slightly younger than the 931 ± 2 Ma U–Pb intrusion age of the igneous complex and a cluster of monazite U–Pb ages at 930–925 Ma in the gneiss complex; it is equivalent to the average regional titanite U–Pb age of 918 ± 2 Ma [Fig. 1(A)].

- (2) A second group of six augen gneiss samples (B185, B198, B308, B630, B613 and B671), located in Rogaland–Vest Agder and Telemark and on both sides of the Cpx-in and Opx-in isograds, gives significantly younger ages between 893 and 855 Ma with an average value of $871 \pm 8 / -10$ Ma; this average is equivalent to available Rb–Sr mineral ages (biotite–whole-rock and K–feldspar: 895–853 Ma) and K–Ar biotite ages (878–853 Ma) in the gneiss complex.

The different geochronometers for which data are available, have accepted closure temperatures ranging from 610 to 100°C, in slowly cooled terranes; these are 610–570°C for the U–Pb system in titanite [effective grain radius of 100 µm; cooling rate of $15\text{--}2^\circ\text{C Ma}^{-1}$; diffusion data of Cherniak (1993)], 550–500°C for the K–Ar system in hornblende (Harrison, 1981) and 360–300°C for the K–Ar and Rb–Sr systems in biotite (Harrison et al., 1985; Giletti, 1991). For the Rb–Sr system in orthoclase, the closure temperature is estimated at 580°C for an effective diffusion domain of 100 µm [cooling rate of 10°C Ma^{-1} ; Cherniak and Watson (1992)]. It ranges from 240 to 100°C for the K–Ar system in plagioclase, mesoperthite and antiperthite (Yu and Morse, 1992).

Considered at the scale of the two terranes, the observed bimodal distribution of $^{40}\text{Ar}/^{39}\text{Ar}$ hornblende ages and the large overlap between the different mineral ages do not converge to any reliable regional cooling path, in the range 610–300°C. The older hornblende ages close to the Rogaland Igneous Complex ($916 \pm 12 / -14$ Ma), are probably not attributable to differential uplift, as no tectonic or suture zone is reported close to the margin of this complex. On the other hand, hornblende ages in the Feda suite

are not correlated to hornblende compositions (e.g. samples B185 and B198 in the young age group versus samples B114 and B195 in the oldest age group), indicating that variation of Ar retentivity linked to hornblende composition are not significant. For the range of composition of amphibole in this suite (Fig. 2), the empirical model of Dahl (1996) predicts a variation of the closure temperature of 10°C at most; this small interval can hardly account for the 75 m.y. spread in observed hornblende ages.

7.2. Hornblende $^{40}\text{Ar}/^{39}\text{Ar}$ ages and M2 parageneses in Rogaland–Vest Agder

In the Feda suite, titanite abundance drops close to the Cpx-in isograd. At higher grade, it only occurs as relict inclusions in K-feldspar and amphibole. The tight grouping of U–Pb ages at 918 ± 2 Ma in these inclusions is interpreted as a cooling age, probably controlled by volume diffusion of Pb [Fig. 1(A); discussion in Bingen and van Breemen (1996)]. On the other hand, evolution of the rare earth element (REE) pattern of apatite indicates that monazite is a breakdown-product of allanite + titanite or allanite + hornblende (Bingen et al., 1996) close to the Cpx-in isograd in this suite. In three hornblende-bearing samples between the Cpx-in and Opx-in isograds, there is a correlation between monazite U–Pb age and the $\text{Cpx}/(\text{Cpx} + \text{Hbl})$ ratio: in the Cpx-rich sample [$\text{Cpx}/(\text{Cpx} + \text{Hbl}) = 0.87$], four monazites plotted at 928–925 Ma whereas in Cpx-poor samples [$\text{Cpx}/(\text{Cpx} + \text{Hbl}) < 0.22$] nine monazites were spread between 1012 and 904 Ma without cluster at 928–925 Ma. These results suggest that monazite + Cpx crystallization linked to hornblende breakdown occurred at 928–925 Ma during M2 metamorphism in some samples (Bingen and van Breemen, in press).

The hornblende $^{40}\text{Ar}/^{39}\text{Ar}$ ages obtained in this study are also correlated with the pyroxene/hornblende ratio and M2 overprinting in the samples. To the east of the Cpx-in isograd, all pyroxene-free samples yield spectra in the $871 \pm 8 / -10$ Ma age group. In the Feda suite to the west of this isograd, samples B195 and B114 with high $\text{Px}/(\text{Px} + \text{Hbl})$ ratios (0.55 and 0.36)

yield ages of 928 ± 16 Ma (B195), and 904 ± 22 or 930 ± 24 Ma (B114) whereas samples B185 and B198 with low $Px/(Px+Hbl)$ ratios (0.22 and 0.19) have apparent ages of 867 ± 2 and 875 ± 20 Ma. In the amphibolites, Cpx-rich-biotite-free sample P1158 showing homogeneous M2 overprinting yields an age of 918 ± 8 Ma. Sample HA54 in which a hornblende-bearing M1 association is replaced locally by a two pyroxene M2 association, gives an age of 910 ± 8 Ma with some excess Ar (intercept age of 902 ± 2 Ma) and pyroxene-poor sample ROG43 showing limited M2 overprinting displays large amount of excess Ar. This age pattern thus indicates that all samples displaying substantial Cpx growth and dehydration during M2 phase, yield hornblende $^{40}Ar/^{39}Ar$ spectra in the $916 \pm 12/-14$ Ma age cluster.

If the age of 928–925 Ma is accepted for pyroxene growth during M2, the hornblende closed for Ar diffusion in the least hydrated samples shortly after M2, simultaneously with the U–Pb system in titanite. Interpretation of these titanite and hornblende data in terms of cooling suggests that M2 was shortly followed by a regional drop of temperature. Using a 850–800°C temperature interval for M2 to the west of the osumilite-in isograd and a 610–500°C interval for the closure of both Ar diffusion in hornblende and Pb diffusion in titanite, a minimum cooling rate of $\sim 15^\circ C Ma^{-1}$ can be derived for the gneiss complex in the core of the domain.

On the other hand, in samples with a mineral association dominated by hornblende + biotite, hornblende yields apparent $^{40}Ar/^{39}Ar$ ages at $871 \pm 8/-10$ Ma or display excess Ar. As the mineral association points to fluid saturated conditions, the probability of interaction between hornblende and pore fluid was thus higher than in the pyroxene-rich samples. Protracted fluid-mediated loss of radiogenic Ar produced in hornblende possibly occurred in samples clustering at $871 \pm 8/-10$ Ma. Introduction of extraneous radiogenic Ar apparently occurred in hornblende-rich amphibolites (mainly ROG43). The role of metamorphic fluid for introducing or removing radiogenic Ar in hornblende in a temperature range close to the closure temperature for Ar diffusion was demonstrated by Cumbest et al.

(1994). Evidence for fluid activity after the blocking of the U–Pb system in titanite is shown in the pyroxene-poor samples of the Feda suite by the crystallization of U-poor hydrothermal monazite at 912–904 Ma [three samples with $Cpx/(Cpx+Hbl) < 0.22$, including B185 and B198]. Whether the cluster of hornblende $^{40}Ar/^{39}Ar$ ages, K–Ar biotite ages and Rb–Sr mineral ages ca 0.87 Ga corresponds to a low-grade, late Sveconorwegian metamorphic or hydrothermal event or to a decrease in the regional cooling rate remains unclear.

7.3. Tectonic history along the Mandal Line

The northern and central sections of the Mandal Line, between the Rogaland–Vest Agder and Telemark terranes, show evidence for ‘early’ ductile shearing and ‘late’ brittle faulting (Sigmond, 1985). The ‘early’ shearing is older than ca 1.14 Ga as the supracrustal Bandak group [zircon U–Pb age: Dahlgren cited in Starmer (1993)], unconformably overlies a 2.5–3 km broad zone of intensely sheared gneisses. The ‘late’ movements are younger than 1.14 Ga; the youngest normal faults cataclastically affect the ca 0.98 Ga post-tectonic granitoids (Sigmond, 1985).

The southernmost part (60 km) of the Mandal Line corresponds to a N–S, ca 4 km broad, amphibolite-facies banded gneiss unit. Mylonitic rocks or faults have not been reported. The spatial distribution, together with the distinct geochemical and geochronological features of two suites of syn-kinematic elongate bodies of augen gneiss situated on both sides of the Mandal Line, the calc-alkaline Feda suite (1.05 Ga) to the west and the more alkaline Fennefoss augen gneiss (1.035 Ga) to the east, show that this section of the line was active between 1.05 and 1.035 Ga. Both terranes were subsequently affected by amphibolite-facies metamorphism, and ductile shearing took place under amphibolite-facies conditions along the banded gneiss unit (Bingen and van Breemen, 1998).

The $^{40}Ar/^{39}Ar$ hornblende ages on both sides of the southern section of the Mandal Line are similar and define an average of $871 \pm 8/-10$ Ma [Fig. 1(B)]. Whatever the exact significance of these hornblende ages may be, the similarity of

hornblende $^{40}\text{Ar}/^{39}\text{Ar}$ ages, titanite U–Pb ages and biotite Rb–Sr ages in the southern parts of Rogaland–Vest Agder and Telemark suggests that these terranes share a common post-orogenic evolution and that no significant differential uplift occurred along the southern section of the Mandal Line (Fig. 5). This conclusion is consistent with a tectonic model involving essentially strike-slip displacements during the last main orogenic phase, as proposed by Starmer (1993) and Bingen and van Breemen (1998) on the basis of structural and geochronological analysis.

7.4. Differential uplift along the Kristiansand–Porsgrunn shear zone

The Kristiansand–Porsgrunn shear zone, which marks the boundary between the Bamble and Telemark terranes, is a polyphase tectonic zone. Its north-eastern section corresponds to a network of ductile mylonite, up to several kilometres in thickness. This network crosscuts the Morkheia monzonite suite intruded at 1132 ± 3 Ma (Heaman and Smalley, 1994), implying that a major phase

of ductile shearing occurred along this zone after 1.13 Ga. The N–S lineation in the Gjerstad augen gneiss, together with the SE dip of the ductile shear zone suggests that Bamble was thrust north-westwards onto Telemark (Starmer, 1993) during Sveconorwegian compressive tectonic phases. The mylonite zone is cut by a late fault zone extending from Kristiansand to Porsgrunn. Crustal relaxation resulted in a normal decompression shearing along this fault zone with downthrow of Bamble relative to Telemark (Starmer, 1993). Late brittle normal faulting affects the Herefoss post-kinematic granite after its intrusion at 926 ± 8 Ma (Andersen, 1997).

Hornblende K–Ar data for 12 samples from the amphibolite- to granulite-facies gneiss complex of the coastal region of Bamble range from 1108 to 965 Ma with an average value of 1034 Ma (Cosca and O’Nions, 1994). The hornblende $^{40}\text{Ar}/^{39}\text{Ar}$ data on the same sample-set (Cosca and O’Nions, 1994) yield an older and more consistent age distribution from 1112 to 1081 Ma with an average value of $1091 + 21/-10$ Ma [Fig. 1(B)]. The similarity of hornblende $^{40}\text{Ar}/^{39}\text{Ar}$ ages and gar-

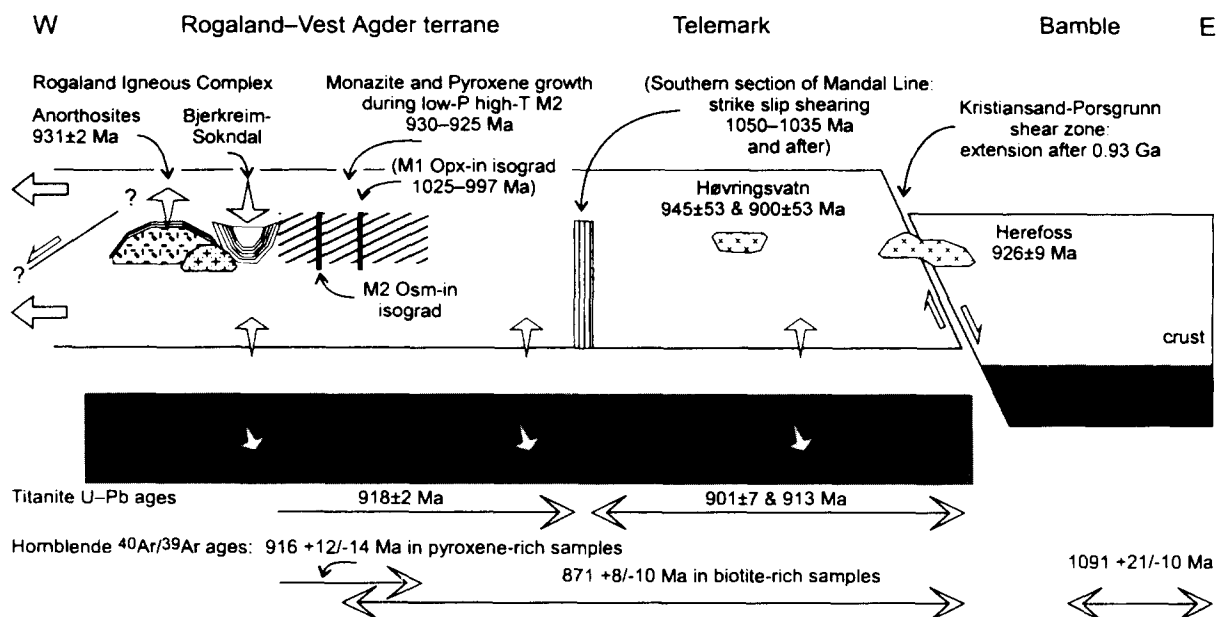


Fig. 5. Interpretative schematic W–E cross sections in the Rogaland–Vest Agder, Telemark and Bamble terranes integrating the hornblende $^{40}\text{Ar}/^{39}\text{Ar}$ ages in a model of post-thickening extension at 0.93–0.92 Ga. See Fig. 1 for legend. The model for intrusion of the Rogaland Igneous Complex is adapted from Schärer et al. (1996).

net-whole-rock Sm–Nd internal isochron age [1098 ± 7 Ma; Kullerud and Dahlgren (1993)] suggests rapid cooling in Bamble ca 1.09 Ga.

In southern Telemark, in the foot wall of the Kristiansand–Porsgrunn shear zone, metamorphic ages are much younger: at ca 10–30 km NW of the shear zone, zircon yields a lower intercept age of $987 + 81 / - 117$ Ma in a ca 1.17 Ga augen gneiss (Bingen and van Breemen, 1998), titanite has U–Pb ages of 913 and 901 ± 7 Ma (Heaman and Smalley, 1994; Bingen and van Breemen, in press) and hornblende in augen gneiss samples B671 and B613 gives $^{40}\text{Ar}/^{39}\text{Ar}$ release spectra at 893 ± 14 , 861 ± 36 and 864 ± 8 Ma, respectively [Fig. 3(H), Fig. 3(F)].

The Hovdefjell charnockitic augen gneiss (sample D84/8) is situated close to the Kristiansand–Porsgrunn shear zone, in the highly strained hanging wall (Fig. 1). This body forms a lens of relatively unshaped gneiss incorporated in the mylonitic network of the shear zone (Starmer, 1991). Although the $^{40}\text{Ar}/^{39}\text{Ar}$ spectrum displays disturbances, hornblende yields a significant $^{40}\text{Ar}/^{39}\text{Ar}$ age of 1030 ± 4 Ma, younger than the samples of the coastal region of Bamble but older than the samples of S. Telemark [Fig. 1(B)].

The contrast in $^{40}\text{Ar}/^{39}\text{Ar}$ hornblende cooling ages between Telemark and Bamble means that the latter was uplifted far earlier and that this differential uplift occurred along the Kristiansand–Porsgrunn shear zone. The intermediate age obtained in the vicinity of the shear zone is consistent with this interpretation. Uplift of Bamble at 1.09 Ga was possibly associated with thrusting of this terrane along the Kristiansand–Porsgrunn shear zone after granulite facies metamorphism (M2). The absence of $^{40}\text{Ar}/^{39}\text{Ar}$ hornblende ages younger than 1.09 Ga and the intrusion of post-tectonic pegmatite bodies at 1.06 Ga (Baadsgaard et al., 1984) in the core of Bamble implies that this terrane was already at a high structural level early in the tectonic evolution of the Sveconorwegian orogeny and that it was not affected by post 1.09 Ga high-grade penetrative events, observed in the western terranes. On the other hand, extensional faulting along Kristiansand–Porsgrunn shear zone after 926 ± 8 Ma, with downthrow of Bamble, probably

played a significant role in bringing the two terranes with different cooling histories to equivalent crustal levels (Fig. 5).

7.5. Hornblende $^{40}\text{Ar}/^{39}\text{Ar}$ ages and Sveconorwegian post-orogenic extension

In the Grenville Province of Laurentia, pulses of massif-type anorthosite and charnockite plutonism are correlated with short-lived (30 m.y.) phases of extension in specific domains of the orogen (Martignole, 1996; Corrigan and Hanmer, 1997). These local phases of thinning of the lithosphere occurred in a globally convergent orogen. In the Sveconorwegian orogen, anorthosite magmatism is largely post-tectonic (0.93 Ga) and, following Romer (1996), could correspond to an event of post-thickening extensional collapse.

Until now, extensional structures and shear zones are not reported in the vicinity of the Rogaland Igneous Complex, and the emplacement mechanism of the anorthosite bodies themselves is not constrained in detail (vertical versus horizontal expansion, diapirism versus ballooning). Anorthosite bodies intruded by ascent of a plagioclase-rich crystal mush (Duchesne et al., 1985). The occurrence of a broad deformed margin at the edge of the Egersund–Ogna anorthosite body indicates that the ascent continued at subsolidus temperatures by solid state ductile deformation. Ascent of anorthosites was coeval with sagging and folding of the Bjerkreim–Sokndal layered intrusion on their margin (Paludan et al., 1994; Schärer et al., 1996). It is premature to define the tectonic setting during intrusion of the igneous complex. The existence of extensional shear zones to the west (offshore) of the Rogaland Igneous Complex cannot be ruled out. In Bamble, normal faulting occurred along the Kristiansand–Porsgrunn shear zone after 0.93 Ga (see above). In the Swedish external domains of the orogen, extensional reactivation and exhumation along the frontal thrust zone—the Protogine Zone—is documented at 927–918 Ma (Andréasson and Dallmeyer, 1995). These two observations suggest that the orogen had globally turned to an extensional regime by 0.93–0.90 Ga.

During an event of post-thickening extension,

the thickened lithospheric mantle can be removed by gravitational collapse or convective thinning, and hot asthenospheric mantle arrives in contact with the crust. Some of the following effects can be produced: elevation and extension of the crust, production of both mafic mantle-derived magma and crustal magma, heat transfer to the crust resulting in an increased geothermal gradient followed by rapid exhumation and cooling, formation of extensional basins with high subsidence rates (Dewey, 1988). Some of these features are consistent with geological observations made in the south of the Rogaland–Vest Agder and Telemark terranes (Fig. 5). Production of large volumes of post-kinematic plutonism (anorthosite and charnockite plutons) occurred in a short time span at 0.93 Ga. The succession of metamorphic phases suggests a coeval thermal pulse at a relatively high level in the crust: M1 regional medium-*P* metamorphism at 1.03–1.00 Ga was followed by high-*T*–low-*P* M2 and M3 phases (5.5–3 kbar) at 0.93–0.92 Ga. The maximum pressure of crystallization of the Bjerkreim–Sokndal intrusion is estimated at 5 kbar (Vander Auwera and Longhi, 1994) indicating that this intrusion was relatively shallow. Hornblende $^{40}\text{Ar}/^{39}\text{Ar}$ and titanite U–Pb geochronology suggest a phase of rapid cooling ($>15^\circ\text{C Ma}^{-1}$) shortly after the thermal pulse in the crust. It is worth noting that fast cooling rates are also documented in the Swedish part of the orogen, in the vicinity of the Mylonite Zone, between 934 and 904 Ma [$6\text{--}15^\circ\text{C Ma}^{-1}$ between 500 and 350°C ; Page et al. (1996)].

8. Conclusions

- (1) In the coastal region of the Bamble terrane, hornblende $^{40}\text{Ar}/^{39}\text{Ar}$ ages cluster at $1091 \pm 21/-10$ Ma. In the south of the Rogaland–Vest Agder and Telemark terranes, they define a bimodal distribution, related to the metamorphic assemblages acquired during high-*T*–low-*P* M2 metamorphism (928–925 Ma). Pyroxene-rich samples, located close to the Rogaland Igneous Complex, yield an average age of $916 \pm 12/-14$ Ma. Hornblende + biotite-rich samples, showing limited M2 overprinting, define a regional age of $871 \pm 8/-10$ Ma. In the least hydrated samples, the hornblende $^{40}\text{Ar}/^{39}\text{Ar}$ ages and titanite U–Pb ages (918 ± 2 Ma) probably record a drop of temperature shortly after intrusion of the Rogaland Igneous Complex (931 ± 2 Ma) and associated M2 metamorphism. In samples with higher fluid content, the $^{40}\text{Ar}/^{39}\text{Ar}$ system was affected probably by interaction with metamorphic fluids during a phase of decreased cooling rate or a late Sveconorwegian metamorphic/hydrothermal phase.
- (2) The southern section of the Mandal Line, the tectonic zone between Rogaland–Vest Agder and Telemark terranes, corresponds to a banded gneiss unit. Shearing took place under amphibolite-facies conditions in this unit at and after 1.05 Ga and was not followed by differential uplift as suggested by the similarity of hornblende $^{40}\text{Ar}/^{39}\text{Ar}$ ages in both terranes. Displacements during the Sveconorwegian orogeny were probably essentially of a strike-slip nature. Sveconorwegian differential movements between Bamble and Telemark are documented. They were accommodated by shearing along the Kristiansand–Porsgrunn shear zone, first by a phase of thrusting younger than 1.13 Ga and then a phase of relaxation, which ended after 0.93 Ga. The hornblende $^{40}\text{Ar}/^{39}\text{Ar}$ data definitely show that high-grade metamorphic phases younger than 1.09 Ga had only limited thermal effect in Bamble.
- (3) The south of the Rogaland–Vest Agder and Telemark terranes were probably affected by an event of post-thickening extension at 0.93–0.92 Ga. The elements for this model are mainly: voluminous mafic (anorthosites) to felsic (charnockites, granites) plutonism tightly grouped in time; high-*T*–low-*P* metamorphism (M2, M3 phases); and fast cooling rates on a regional scale after these events.

Acknowledgment

B. Bingen and A. Boven both acknowledge a postdoctoral research fellowship from the Belgian

National Fund for Scientific Research. J.R. Wijbrans carried out $^{40}\text{Ar}/^{39}\text{Ar}$ analyses on samples provided by J.B.H. Jansen, while being funded by an ANU research fellowship. I. McDougall kindly made available his argon laboratory for analysis of these samples. The staff of the BR2 reactor BNRC at Mol (Belgium) is thanked for performing the neutron irradiation experiments and dosimetry analyses. B. Bingen and A. Boven finished the preparation of the manuscript when working at the University of Oslo and the Open University (Milton Keynes); thanks are due to H. Austrheim and S.P. Kelley. C. Maijer, P. Pasteels and P. Padget carefully read different versions of the paper. Constructive reviews were provided by L.M. Page and R.G. Park. The present work was supported by a FKFO-FRFC grant to D. Demaiffe and P. Pasteels. The contribution of J.R. Wijbrans is covered by NSG 970153.

Appendix A: Short sample description

9.1. B114

Grey augen gneiss; $\text{SiO}_2 = 66.3 \text{ wt\%}$; $\text{Mg\#} = 65$ ($100 \times \text{MgO}/(\text{MgO} + \text{FeO})$ atomic ratio); UTM coordinate: x 3721, y 64622.

Mineralogy Pl, Qtz, Kfs (Or), Cpx, olive-green Hbl, Bt, Fe–Ti oxides, Ap, Zrn; Cpx commonly has Hbl and Bt inclusions.

Secondary features Local partial alteration of Pl and Cpx, local secondary Ep, very local partial chloritization of Hbl.

9.2. B185

Grey augen gneiss; $\text{SiO}_2 = 63.0\%$; $\text{Mg\#} = 66$; UTM: 3655 64932.

Mineralogy Pl, Qtz, Kfs (Or), Cpx, olive-green Hbl, Bt, Fe–Ti oxides, Ap, Zrn.

Secondary features Local partial alteration of Pl and Cpx, local secondary Ep.

9.3. B195

Grey augen gneiss; $\text{SiO}_2 = 66.0\%$; $\text{Mg\#} = 66$; UTM: 3569 64711.

Mineralogy Pl, Qtz, Kfs (Or), Opx, Cpx, brown to olive-green Hbl, Bt, Fe–Ti oxides, Ap, Zrn.

Secondary features Important alteration of Opx, very local alteration of Pl.

9.4. B198

Grey augen gneiss; $\text{SiO}_2 = 64.9\%$; $\text{Mg\#} = 67$; UTM: 3626 64791.

Mineralogy Pl, Qtz, Kfs (Or), Opx, Cpx, brown to olive-green Hbl, Bt, Fe–Ti oxides, Ap, Zrn; Hbl commonly twinned.

Secondary features Common alteration of Opx, rare local partial chloritization of Bt.

9.5. B308

Green metacharnockite-augen gneiss; $\text{SiO}_2 = 68.8\%$; $\text{Mg\#} = 30$; UTM: 3881 64602.

Mineralogy Pl, Qtz, Kfs (Or), deep olive-green Hbl, Bt, Fe–Ti oxides, Aln, Ap, Zrn, pyroxene ghosts (?); patches of Opx seen in outcrop.

Secondary features Locally Hbl displays 10–30 μm patches or fractures filled with red and opaque oxides or rarely chlorite, common partial chloritization of Bt, total alteration of pyroxene.

9.6. B613

Grey augen gneiss; $\text{SiO}_2 = 62.1\%$; $\text{Mg\#} = 53$; UTM: 4286 64912.

Mineralogy Pl, Qtz, Kfs (Or + locally Mc), olive-green to bluish-green Hbl, Bt, Fe–Ti oxides, Aln–Ep, Ttn, Cal, Ap, Zrn.

9.7. B630

Grey augen gneiss; $\text{SiO}_2 = 65.6\%$; $\text{Mg\#} = 65$; UTM: 4118 64578.

Mineralogy Pl, Qtz, Kfs (Mc), olive-green to green Hbl, Bt, Fe–Ti oxides, Ttn, Aln, Ap, Zrn.

Secondary features Locally Hbl displays 20–40 μm patches or fractures filled with chlorite, common partial chloritization of Bt, local partial alteration of Pl.

9.8. B671

Pink augen gneiss; $\text{SiO}_2 = 74.0\%$; $\text{Mg\#} = 31$; UTM: 4363 64388.

Mineralogy Pl, Qtz, Kfs (Or + Mc), olive-green to bluish-green Hbl, Bt, Fe–Ti oxides, Aln, Ttn, Ap, Zrn; Hbl locally zoned on the edge to more bluish colour.

Secondary features Very local partial alteration of Pl.

9.9. D84/8

Green metacharnockite-augen gneiss; $63 < \text{SiO}_2 < 70\%$; UTM: 4802 65070.

Matrix made of millimetre-sized granoblastic texture with local granulation of Pl.

Mineralogy Pl, Qtz, Kfs (Or), ghosts of pyroxene, olive-green to green Hbl, Bt, Fe–Ti oxides, Aln, Ap, Zrn; Bt and Hbl locally surrounded by Bt + Qtz symplectite, Hbl locally zoned on the edge to bluish colour.

Secondary features Total alteration of pyroxene, local partial chloritization of Bt.

9.10. HA54

Biotite–pyroxene amphibolite; UTM: 3175 65142.

Mineralogy Pl, Opx, Cpx, brown to olive-green Hbl, Bt, Fe–Ti oxides, Ap; pyroxenes commonly includes Hbl and Bt; patchy replacement of Hbl + Bt + two pyroxenes association by two pyroxenes + oxydes association.

Secondary features Very local partial alteration of Pl.

9.11. P1158

Pyroxene amphibolite; UTM: 38142 645193.

Major minerals Pl, Cpx, olive-green Hbl, Fe–Ti oxides, Ap.

Secondary features Very local partial alteration of Pl.

9.12. ROG43

Biotite amphibolite; UTM: 3626 64772.

Mineralogy Pl, olive-green Hbl, Bt, pyroxene (uncommon), Qtz (rare), Ap.

Secondary features Almost total retrogression of pyroxene.

References

- Andersen, T., 1997. Radiogenic isotope systematics of the Herefoss granite, South Norway: an indicator of Sveconorwegian (Grenvillian) crustal evolution in the Baltic shield. *Chem. Geol.* 135, 139–158.
- Andréasson, P.G., Dallmeyer, R.D., 1995. Tectonothermal evolution of high-alumina rocks within the Protogine Zone, southern Sweden. *J. Metam. Geol.* 13, 461–474.
- Baadsgaard, H., Chaplin, C., Griffin, W.L., 1984. Geochronology of the Glossetheia pegmatite, Froland, southern Norway. *Norsk Geol. Tidsskr.* 64, 111–119.
- Baksi, A.K., Archibald, D.A., Farrar, E., 1996. Intercalibration of $^{40}\text{Ar}/^{39}\text{Ar}$ dating standards. *Chem. Geol.* 129, 307–324.
- Bingen, B., 1988. Origine magmatique et évolution métamorphique de la série des gneiss ocellés de Norvège méridionale: études pétrologique, géochimique et isotopique. PhD Thesis, Université Libre de Bruxelles, Belgium.
- Bingen, B., van Breemen, O., 1996. U–Pb titanite geochronology in Rogaland–Vest Agder (SW Norway): regional temperature at the time of emplacement of the Rogaland anorthosites. In: Demaiffe, D. (Ed.), *Petrology and Geochemistry of Magmatic Suites of Rocks in the Continental and Oceanic Crust*. A volume dedicated to J. Michot. ULB-MRAC, pp. 145–159.
- Bingen, B., van Breemen, O., 1998. Tectonic regimes and terrane boundaries in the high-grade Sveconorwegian belt of SW Norway, inferred from U–Pb zircon geochronology and geochemical signature of augen gneiss suites. *J. Geol. Soc. London*, 155, 143–154.
- Bingen, B., van Breemen, O., U–Pb monazite ages in amphibolite- to granulite-facies orthogneisses reflect hydrous mineral breakdown reactions: Sveconorwegian Province of SW Norway. *Contrib. Min. Petrol.*, in press.
- Bingen, B., Demaiffe, D., Hertogen, J., 1990. Evolution of feldspars at the amphibolite–granulite facies transition in augen gneisses (SW Norway): geochemistry and Sr isotopes. *Contrib. Mineral. Petrol.* 105, 275–288.
- Bingen, B., Demaiffe, D., Hertogen, J., 1996. Redistribution of rare-earth elements, Th and U over accessory minerals in the course of amphibolite to granulite facies metamorphism: the role of apatite and monazite in orthogneisses from SW Norway. *Geochim. Cosmochim. Acta* 60, 1341–1354.
- von Blanckenburg, F., Villa, I.M., 1988. Argon retentivity and argon excess in amphiboles from the garbenschiefer of the Western Tauern Window, Eastern Alps. *Contrib. Mineral. Petrol.* 100, 1–11.
- Boven, A., Pasteels, P., Demaiffe, D., Bingen, B., Punzalan, L., 1996. ^{40}Ar – ^{39}Ar release spectra on plagioclases from the Rogaland anorthosite complex (SW Norway). In: Demaiffe, D. (Ed.), *Petrology and Geochemistry of Magmatic Suites of Rocks in the Continental and Oceanic Crust*. A volume dedicated to J. Michot. ULB-MRAC, pp. 83–97.
- Boven, A., Pasteels, P., Punzalan, L., Demaiffe, D., Bingen, B., Kelley, S.P., submitted. Insights in the K and Ar migration within plagioclases of the Rogaland igneous complex through $^{40}\text{Ar}/^{39}\text{Ar}$ dating.
- Cherniak, D.J., 1993. Lead diffusion in titanite and preliminary results on the effects of radiation damage on Pb transport. *Chem. Geol.* 110, 177–194.
- Cherniak, D.J., Watson, E.B., 1992. A study of strontium diffusion in K-feldspar, Na–K feldspar and anorthite using

- Rutherford backscattering spectroscopy. *Earth Planet. Sci. Lett.* 113, 411–425.
- Corrigan, D., Hanmer, S., 1997. Anorthositic and related granulites in the Grenville orogen: a product of convective thinning of the lithosphere? *Geology* 25, 61–64.
- Cosca, M.A., O'Nions, R.K., 1994. A re-examination of the influence of composition on argon retentivity in metamorphic calcic amphiboles. *Chem. Geol.* 112, 39–56.
- Cumbest, R.J., Johnson, E.L., Onstott, T.C., 1994. Argon composition of metamorphic fluids: implications for $^{40}\text{Ar}/^{39}\text{Ar}$ geochronology. *Geol. Soc. Am. Bull.* 106, 942–951.
- Dahl, P.S., 1996. The effects of composition on retentivity of argon and oxygen in hornblende and related amphiboles: a field-tested empirical model. *Geochim. Cosmochim. Acta* 60, 3687–3700.
- Demaiffe, D., Michot, J., 1985. Isotope geochronology of the Proterozoic crustal segment of southern Norway: a review. In: Tobi, A.C., Touret, J.L. (Eds.), *The Deep Proterozoic Crust in the North Atlantic Provinces*. NATO-ASI C158. NATO-ASI, Reidel, pp. 411–433.
- Dewey, J.F., 1988. Extensional collapse of orogens. *Tectonics* 7, 1123–1139.
- Dodson, M.H., 1973. Closure temperature in cooling geochronological and petrological systems. *Contrib. Mineral. Petrol.* 40, 259–274.
- Duchesne, J.-C., Maquil, R., Demaiffe, D., 1985. The Rogaland anorthositic: facts and speculations. In: Tobi, A.C., Touret, J.L. (Eds.), *The Deep Proterozoic Crust in the North Atlantic Provinces*. NATO-ASI C158. NATO-ASI, Reidel, pp. 449–476.
- Falkum, T., 1985. Geotectonic evolution of southern Scandinavia in light of a late-Proterozoic plate-collision. In: Tobi, A.C., Touret, J.L. (Eds.), *The Deep Proterozoic Crust in the North Atlantic Provinces*. NATO-ASI C158. NATO-ASI, Reidel, pp. 309–322.
- Giletti, B.J., 1991. Rb and Sr diffusion in alkali feldspars, with implications for cooling histories of rocks. *Geochim. Cosmochim. Acta* 55, 1331–1343.
- de Haas, G.-J., Verschure, R.H., Maijer, C., 1993. Isotopic constraints on the timing of crustal accretion of the Bamble Sector, Norway, as evidenced by coronitic gabbros. *Precambrian Res.* 64, 403–417.
- Harrison, T.M., 1981. Diffusion of ^{40}Ar in hornblende. *Contrib. Mineral. Petrol.* 78, 324–331.
- Harrison, T.M., McDougall, I., 1981. Excess ^{40}Ar in metamorphic rocks from Broken Hill, New South Wales: implications for $^{40}\text{Ar}/^{39}\text{Ar}$ age spectra and the thermal history of the region. *Earth Planet. Sci. Lett.* 55, 123–149.
- Harrison, T.M., Duncan, I., McDougall, I., 1985. Diffusion of ^{40}Ar in biotite: temperature, pressure and compositional effects. *Geochim. Cosmochim. Acta* 49, 2461–2468.
- Heaman, L.M., Smalley, P.C., 1994. A U–Pb study of the Morkheia Complex and associated gneisses, south Norway: implications for disturbed Rb–Sr systems and for the temporal evolution of Mesoproterozoic magmatism in Laurentia. *Geochim. Cosmochim. Acta* 58, 1899–1911.
- Holland, T.J., Babu, E.V., Waters, D.J., 1996. Phase relations of osumilite and dehydration melting in pelitic rocks: a simple thermodynamic model for the KFMASH system. *Contrib. Mineral. Petrol.* 124, 383–394.
- Jansen, J.B.H., Blok, R.J., Bos, A., Scheelings, M., 1985. Geothermometry and geobarometry in Rogaland and preliminary results from the Bamble area, S. Norway. In: Tobi, A.C., Touret, J.L. (Eds.), *The Deep Proterozoic Crust in the North Atlantic Provinces*. NATO-ASI C158. NATO-ASI, Reidel, pp. 499–516.
- Kelley, S.P., Turner, G., 1991. Laser probe $^{40}\text{Ar}/^{39}\text{Ar}$ measurements of loss profiles within individual hornblende grains from the Giant Range Granite, northern Minnesota, USA. *Earth Planet. Sci. Lett.* 107, 634–648.
- Knudsen, T.-L., Petrology and geothermobarometry of granulite facies metapelites from the Hisøy-Torungen area, south Norway: new data on the Sveconorwegian $P-T-t$ path of the Bamble sector. 1996. *J. Metam. Geol.* 14, 267–287.
- Kullerød, L., Dahlgren, S.H., 1993. Sm–Nd geochronology of Sveconorwegian granulite facies mineral assemblages in the Bamble shear belt, south Norway. *Precambrian Res.* 64, 389–402.
- Lee, J.K.W., 1995. Multipath diffusion in geochronology. *Contrib. Mineral. Petrol.* 120, 60–82.
- Lee, J.K.W., Onstott, T.C., Cashman, K.V., Cumbest, R.J., Johnson, D., 1991. Incremental heating of hornblende in vacuo: implications for $^{40}\text{Ar}/^{39}\text{Ar}$ geochronology and the interpretation of thermal histories. *Geology* 19, 872–876.
- Maijer, C., 1987. The metamorphic envelope of the Rogaland intrusive complex. In: Maijer, C., Padget, P. (Eds.), *The Geology of Southernmost Norway: An Excursion Guide*. Norges Geologiske Undersøkelse, Special Publication No. 1. Norges Geologiske Undersøkelse, Trondheim, Norway, pp. 68–73.
- Maijer, C., Verschure, R.H., Visser, D., 1994. Strontium isotope study of two supposed satellite massifs of the Egersund Anorthosite Complex: the Sjelset Igneous Complex and the Undheim Leuconorite. *Norsk Geol. Tidsskr.* 74, 58–69.
- Martignole, J., 1996. Tectonic setting of anorthositic complexes of the Grenville Province, Canada. In: Demaiffe, D. (Ed.), *Petrology and Geochemistry of Magmatic Suites of Rocks in the Continental and Oceanic Crust*. A volume dedicated to J. Michot. ULB-MRAC, pp. 3–18.
- Nijland, T.G., Maijer, C., 1993. The regional amphibolite to granulite facies transition at Arendal, Norway: evidence for a thermal dome. *Neues Jahrbuch Mineral. Abh.* 165, 191–221.
- Page, L.M., Möller, C., Johansson, L., 1996. $^{40}\text{Ar}/^{39}\text{Ar}$ geochronology across the Mylonite Zone and the Southwestern Granulite Province in the Sveconorwegian Orogen of S. Sweden. *Precambrian Res.* 79, 239–259.
- Paludan, J., Hansen, U.B., Olesen, N.O., 1994. Structural evolution of the Precambrian Bjerkeim–Sokndal intrusion, South Norway. *Norsk Geol. Tidsskr.* 74, 185–198.
- Pasteels, P., Demaiffe, D., Michot, J., 1979. U–Pb and Rb–Sr geochronology of the eastern part of the south Rogaland igneous complex, southern Norway. *Lithos* 12, 199–208.
- Pedersen, S., 1981. Rb–Sr age determinations on late

- Proterozoic granitoids from the Evje area, South Norway. *Bull. Geol. Soc. Denmark* 29, 129–143.
- Romer, R.L., 1996. Contiguous Laurentia and Baltica before the Grenvillian–Sveconorwegian orogeny? *Terra Nova* 8, 173–181.
- Schärer, U., Wilmart, E., Duchesne, J.-C., 1996. The short duration and anorogenic character of anorthosite magmatism: U–Pb dating of the Rogaland complex, Norway. *Earth Planet. Sci. Lett.* 139, 335–350.
- Sigmond, E.M., 1985. The Mandal–Ustaoset line, a newly discovered major fault zone in south Norway. In: Tobi, A.C., Touret, J.L. (Eds.), *The Deep Proterozoic Crust in the North Atlantic Provinces*. NATO-ASI C158. NATO-ASI, Reidel, pp. 323–331.
- Starmer, I.C., 1991. The Proterozoic evolution of the Bamble sector shear belt, southern Norway: correlations across southern Scandinavia and the Grenvillian controversy. *Precambrian Res.* 49, 107–139.
- Starmer, I.C., 1993. The Sveconorwegian orogeny in southern Norway, relative to deep crustal structures and events in the North Atlantic Proterozoic Supercontinent. *Norsk Geol. Tidsskr.* 73, 109–132.
- Steiger, R.H., Jäger, E., 1977. Subcommittee on geochronology: convention on the use of decay constants in geo- and cosmochronology. *Earth Planet. Sci. Lett.* 36, 359–362.
- Tobi, A.C., Hermans, G.A., Maijer, C., Jansen, J.B.H., 1985. Metamorphic zoning in the high-grade Proterozoic of Rogaland–Vest Agder, SW Norway. In: Tobi, A.C., Touret, J.L. (Eds.), *The Deep Proterozoic Crust in the North Atlantic Provinces*. NATO-ASI C158. NATO-ASI, Reidel, pp. 477–497.
- Vander Auwera, J., 1993. Diffusion controlled growth of pyroxene-bearing margins on amphibolite bands in the granulite facies of Rogaland (southwestern Norway): implications for granulite formation. *Contrib. Mineral. Petrol.* 114, 203–220.
- Vander Auwera, J., Longhi, J., Experimental study of a jotunite (hypersthene monzodiorite): constraints on the parent magma composition and crystallization conditions (*P*, *T*, *fO₂*) of the Bjerkreim–Sokndal layered intrusion (Norway). 1994. *Contrib. Mineral. Petrol.* 118, 60–78.
- Verschure, R.H., 1985. Geochronological framework for the late-Proterozoic evolution of the Baltic shield in south Scandinavia. In: Tobi, A.C., Touret, J.L. (Eds.), *The Deep Proterozoic Crust in the North Atlantic Provinces*. NATO-ASI C158. NATO-ASI, Reidel, pp. 381–410.
- Verschure, R.H., Andriessen, P.A.M., Boelrijk, N.A.M., Hebeda, E.H., Maijer, C., Priem, H.N.A., Verdurmen, E.A.T., 1980. On the thermal stability of Rb–Sr and K–Ar biotite systems: evidence from coexisting Sveconorwegian (ca 870 Ma) and Caledonian (ca 400 Ma) biotites in SW Norway. *Contrib. Mineral. Petrol.* 74, 245–252.
- Wartho, J.A., 1995. Apparent argon diffusive loss ⁴⁰Ar/³⁹Ar age spectra in amphiboles. *Earth Planet. Sci. Lett.* 134, 393–407.
- Wielens, J.B., Andriessen, P.A.M., Boelrijk, N.A.M., Hebeda, E.H., Priem, H.N.A., Verdurmen, E.A.T., Verschure, R.H., 1981. Isotope geochronology in the high-grade metamorphic Precambrian of southwestern Norway: new data and reinterpretations. *Norges Geol. Undersøkelse Bull.* 359, 1–30.
- Wijbrans, J.R., McDougall, I., 1987. On the metamorphic history of an Archaean granitoid greenstone terrane, East Pilbara, Western Australia, using the ⁴⁰Ar/³⁹Ar spectrum technique. *Earth Planet. Sci. Lett.* 84, 226–242.
- Yu, Y., Morse, S.A., 1992. Age and cooling history of the Kiglapait intrusion from an ⁴⁰Ar/³⁹Ar study. *Geochim. Cosmochim. Acta* 56, 2471–2485.
- Zhou, X.Q., Bingen, B., Demaiffe, D., Liégeois, J.-P., Hertogen, J., Weis, D., Michot, J., 1995. The 1160 Ma old Hidderskog meta-charnockite: implications of this A-type pluton for the Sveconorwegian belt in Vest Agder (SW Norway). *Lithos* 36, 51–66.